

1 **Muscleblind regulates *Drosophila Dscam2* cell-type-specific alternative splicing**

2 Joshua Shing Shun Li and S. Sean Millard.

3 School of Biomedical Sciences, The University of Queensland, Brisbane, 4072,

4 Australia.

5 Correspondence: [s.millard@uq.edu.au](mailto:s.millard@uq.edu.au)

6

7 **Summary**

8 **Alternative splicing of genes increases the number of distinct proteins in a cell.**

9 **In the brain it is highly prevalent, presumably because proteome diversity is**  
10 **crucial for establishing the complex circuitry between trillions of neurons. To**  
11 **provide individual cells with different repertoires of protein isoforms, however,**  
12 **this process must be regulated. Previously, we found that the mutually exclusive**  
13 **alternative splicing of *Drosophila Dscam2* exon 10A and 10B is tightly regulated**  
14 **and crucial for maintaining axon terminal size, dendritic morphology and**  
15 **synaptic numbers. Here, we show that *Drosophila muscleblind (mbl)*, a**  
16 **conserved splicing factor implicated in myotonic dystrophy, controls *Dscam2***  
17 **alternative splicing. Removing *mbl* from cells that normally express isoform B**  
18 **induces the expression of isoform A and eliminates the expression of B,**  
19 **demonstrating that Mbl represses one alternative exon and selects the other.**  
20 **Consistent with these observations, we show that *mbl* expression is cell-type-**  
21 **specific and correlates with the expression of isoform B. Our study demonstrates**  
22 **how cell-type-specific expression of a splicing factor can provide neurons with**  
23 **unique protein isoforms.**

24

25

## 26 **Introduction**

27 Alternative splicing occurs in approximately 95% of human genes and generates  
28 proteome diversity much needed for brain wiring (Pan et al., 2008; Wang et al.,  
29 2008). Specifying neuronal connections through alternative splicing would require  
30 regulated expression of isoforms with unique functions in different cell types to carry  
31 out distinct processes. Although there are some examples of neuronal cell-type-  
32 specific isoform expression (Bell et al., 2004; Iijima et al., 2014; Lah et al., 2014;  
33 Norris et al., 2014; Schreiner et al., 2014; Tomioka et al., 2016), the mechanisms  
34 underlying these deterministic splicing events remain understudied. This is due, in  
35 part, to the technical difficulties of assessing isoform expression at the single cell  
36 level. Another obstacle is that most splicing regulators are proposed to be  
37 ubiquitously expressed (Nilsen and Graveley, 2010), therefore it is not immediately  
38 clear how cell-type specific expression would be achieved. For example, the broadly  
39 expressed SR and heterogeneous nuclear ribonucleoproteins (hnRNPs) typically have  
40 opposing activities, and the prevalence of splice site usage is thought to be controlled  
41 by their relative abundances within the cell (Blanchette et al., 2009). There are many  
42 notable examples where splicing regulators are expressed in a tissue-specific manner  
43 (Calarco et al., 2009; Kuroyanagi et al., 2006; Markovtsov et al., 2000; Ohno et al.,  
44 2008; Underwood et al., 2005; Warzecha et al., 2009), but tissues contain numerous  
45 cell types and regulation at this level does not address how cell-type-specific  
46 alternative splicing is achieved.

47

48 In *Drosophila*, *Dscam2* is a cell recognition molecule that mediates self- and cell-  
49 type-specific avoidance (tiling) (Millard et al., 2007; Millard et al., 2010). Mutually  
50 exclusive alternative splicing of exon 10A or 10B produces two isoforms with

51 biochemically unique extracellular domains (Millard et al., 2007). Previously, we  
52 found that the splicing of *Dscam2* is cell-type-specific (Lah et al., 2014). This  
53 deterministic splicing is crucial for the proper development of axon terminal size,  
54 dendrite morphology and synaptic numbers (Kerwin et al., 2018; Lah et al., 2014; Li  
55 et al., 2015). Although the functional consequences of disrupting regulated *Dscam2*  
56 alternative splicing have been demonstrated, what regulates this process remained  
57 unclear. Here, we conducted an RNAi screen and identified *muscleblind* (*mbl*) as a  
58 regulator of *Dscam2* alternative splicing. Loss-of-function (LOF) and overexpression  
59 (OE) studies suggest that Mbl acts both as a splicing repressor of *Dscam2* exon 10A  
60 and as an activator of exon 10B (hereafter *Dscam2.10A* and *Dscam2.10B*). Consistent  
61 with this finding, *mbl* expression is cell-type-specific and correlates with the  
62 expression of *Dscam2.10B*. Driving *mbl* in mushroom body neurons that normally  
63 select isoform A, induces the expression of isoform B and generates a phenotype  
64 similar to that observed in animals that express a single isoform of *Dscam2*. Although  
65 the *mbl* gene is itself alternatively spliced, we found that selection of *Dscam2.10B*  
66 does not require a specific Mbl isoform and that human MBNL1 can also regulate  
67 *Dscam2* alternative splicing. Our study demonstrates that mutually exclusive splicing  
68 of *Dscam2* is regulated by the cell-type-specific expression of a highly conserved  
69 RNA binding protein, Mbl.

70

71

## 72 **Results**

### 73 **An RNAi screen identifies *mbl* as a repressor of *Dscam2* exon 10A selection**

74 We reasoned that the neuronal cell-type-specific alternative splicing of *Dscam2* is  
75 likely regulated by RNA binding proteins, and that we could identify these regulators  
76 by knocking them down in a genetic background containing an isoform reporter. In  
77 photoreceptors (R cells) of third instar larvae, *Dscam2.10B* is selected whereas the  
78 splicing of *Dscam2.10A* is repressed (Lah et al., 2014; Tadros et al., 2016). Given that  
79 quantifying a reduction in *Dscam2.10B* isoform reporter levels is challenging  
80 compared to detecting the appearance of *Dscam2.10A* in cells where it is not normally  
81 expressed, we performed a screen for repressors of isoform A in R cells.

82

83 To knock down RNA binding proteins, the *glass* multimer reporter (*GMR*)-*GAL4* was  
84 used to drive RNAi transgenes selectively in R cells. Our genetic background  
85 included *UAS-Dcr-2* to increase RNAi efficiency (Dietzl et al., 2007) and *GMR-GFP*  
86 to mark the photoreceptors independent of the *Gal4/UAS* system (Brand and  
87 Perrimon, 1993). Lastly, a *Dscam2.10A-LexA* reporter driving *LexAOp*-myristolated  
88 tdTomato (hereafter *Dscam2.10A>tdTom*; Fig. 1A) was used to visualize isoform A  
89 expression (Lai and Lee, 2006; Tadros et al., 2016). As expected,  
90 *Dscam2.10B>tdTom* was detected in R cell projections in the lamina plexus as well as  
91 in their cell bodies in the eye-disc, whereas *Dscam2.10A>tdTom* was not (Fig. 1C-  
92 1D). Overexpression of Dcr-2 in R cells did not perturb the repression of  
93 *Dscam2.10A* (Fig 1O). We knocked down ~160 genes using ~250 RNAi lines (Fig 1B  
94 and Table S1) and identified two independent RNAi lines targeting *mbl* that caused  
95 aberrant expression of *Dscam2.10A* in R cells where it is normally absent (Fig 1F,  
96 1O). The penetrance increased when animals were reared at a higher temperature of



97 29°C, which is more favorable for Gal4 (Mondal et al., 2007; Ni et al., 2008) (Fig  
98 1O).

99

100 Mbl-family proteins possess evolutionarily conserved tandem CCCH zinc-finger  
101 domains through which they bind pre-mRNA. Vertebrate Mbl family members are  
102 involved in tissue-specific splicing and have been implicated in myotonic dystrophy  
103 (Pascual et al., 2006). Formerly known as *mindmelt*, *Drosophila mbl* was first  
104 identified in a second chromosome *P*-element genetic screen for embryonic defects in  
105 the peripheral nervous system (Kania et al., 1995). *Mbl* produces multiple isoforms  
106 through alternative splicing (Begemann et al., 1997; Irion, 2012), and its function has  
107 been most extensively characterized in fly muscles where both hypomorphic  
108 mutations and sequestration of the protein by repeated CUG sequences within an  
109 mRNA lead to muscle defects (Artero et al., 1998; Llamusi et al., 2013). To validate  
110 the RNAi phenotype, we tested *Dscam2.10A>tdTom* expression in *mbl* loss-of-  
111 function (LOF) mutants. Since *mbl* LOF results in lethality, we first conducted  
112 complementation tests on six *mbl* mutant alleles to identify viable hypomorphic  
113 combinations. These included two alleles created previously via imprecise *P*-element  
114 excision (*mbl<sup>e127</sup>* and *mbl<sup>e27</sup>*; Begemann et al. 1997) two MiMIC splicing traps  
115 (*mbl<sup>MI00976</sup>* and *mbl<sup>MI04093</sup>*; (Venken et al., 2011) and two 2<sup>nd</sup> chromosome deficiencies  
116 (*Df(2R)BSC154* and *Df(2R)Exel6066*; Fig 1F-1G). Consistent with previous reports,  
117 the complementation tests confirmed that the majority of the alleles were lethal over  
118 one another (Fig 1G) (Kania et al., 1995). However, we identified two *mbl*  
119 transheterozygous combinations that were partially viable and crossed these into a  
120 *Dscam2.10A>tdTom* reporter background. Both *mbl<sup>e127</sup>/mbl<sup>MI00976</sup>* and  
121 *mbl<sup>MI04093</sup>/mbl<sup>MI00976</sup>* animals presented aberrant *Dscam2.10A* expression in R cells

122 when compared to heterozygous and wild-type controls (Fig 1H-O). *Mbl* mutant  
123 mosaic clones also exhibited aberrant *Dscam2.10A>tdTom* expression in R cells (Fig  
124 S1A-S1F). The weakest allele, *mbl*<sup>M100976</sup>, which removes only a proportion of the *mbl*  
125 isoforms, was the only exception (Fig S1E-S1F).

126

127 One alternative explanation of how *Dscam2.10A>tdTom* expression could get  
128 switched-on in *mbl* mutants, is through exon 10 skipping. Removing both alternative  
129 exons simultaneously does not result in a frameshift mutation, and since the Gal4 in  
130 our reporters is inserted directly downstream of the variable exons (in exon 11), it  
131 would still be expressed. To test this possibility, we amplified *Dscam2* sequences  
132 between exon 9 and 11 in *mbl*<sup>e127</sup>/*mbl*<sup>M100976</sup> transheterozygous animals using RT-PCR.  
133 In both control and *mbl* LOF mutants, we detected RT-PCR products (~690bp) that  
134 corresponded to the inclusion of exon 10 (A or B) and failed to detect products  
135 (~390bp) that would result from exon 10 skipping (Fig 1P). This suggested that Mbl  
136 is not involved in the splicing fidelity of *Dscam2.10* but rather in the selective mutual  
137 exclusion of its two isoforms. To assess whether the ratios of the two isoforms were  
138 changing in the *mbl* hypomorphic mutants, we cut the exon 10 RT-PCR products with  
139 the *ClaI* restriction enzyme that only recognizes exon 10A. Densitometric analysis  
140 then allowed us to semi-quantitatively compare the relative levels of both isoforms.  
141 There was ~25% increase in the level of exon 10A inclusion in *mbl*<sup>e127</sup>/*mbl*<sup>M100976</sup>  
142 animals compared to controls (Fig 1P), consistent with the derepression we observed  
143 in our 10A reporter lines. To determine whether Mbl was specifically regulating  
144 *Dscam2* exon 10 mutually exclusive splicing, we assessed other *Dscam2* alternative  
145 splicing events. These included an alternative 5' splice site selection of *Dscam2* exon  
146 19 and the alternative last exon (ALE) selection of exon 20 (Fig S2A). The expression

147 of these different isoforms was unchanged in *mbl* hypomorphic mutants (Fig S2B).  
148 Together, our results indicate that Mbl is an essential splicing factor that specifically  
149 represses *Dscam2.10A*.

150

### 151 ***Mbl* is necessary for the selection of *Dscam2* exon 10B**

152 Since *Dscam2* exon 10 isoforms are mutually exclusively spliced, we predicted that  
153 selection of exon 10A would lead to the loss of exon 10B selection. To test this, we  
154 conducted mosaic analysis with a repressible cell marker (MARCM) (Lee and Luo,  
155 1999) to analyse *Dscam2.10B* expression in *mbl* mutant clones. In late third instar  
156 brains, clones homozygous (GFP-positive) for *mbl*<sup>E127</sup> and *mbl*<sup>E27</sup> exhibited a dramatic  
157 reduction in *Dscam2.10B>tdTom* expression in R cell axons projecting to the lamina  
158 plexus compared to controls (Fig 2B, C, E). The absence of *Dscam2.10B>tdTom* in  
159 *mbl* mutant clones was more striking during pupal stages (Fig 2D), suggesting that  
160 perdurance of Mbl could explain the residual signal observed in third instar animals.  
161 These results reveal that *mbl* is cell-autonomously required for the selection of the  
162 *Dscam2.10B* isoform.

163

### 164 **Cell-type-specific *mbl* expression is transcriptionally regulated**

165 Previous studies have reported that *mbl* is expressed in third instar eye-discs and  
166 muscles (Artero et al., 1998; Brouwer et al., 1997). Since *mbl* LOF results in both the  
167 production of *Dscam2.10A* and the loss of *Dscam2.10B*, we predicted that *mbl*  
168 expression would correlate with the presence of isoform B. To test this, we  
169 characterized several *mbl* reporters (Fig S3A). We analyzed three enhancer trap  
170 strains (transcriptional reporters) inserted near the beginning of the *mbl* gene  
171 (*mbl*<sup>K01212</sup>-*LacZ*, *mbl*<sup>NP1161</sup>-*Gal4* and *mbl*<sup>NP0420</sup>-*Gal4*), as well as a splicing trap line

172 generated by the Trojan-mediated conversion of a *mbl* MiMIC (Minos Mediated  
173 Integration Cassette) insertion (Fig S2A, *mbl*<sup>MiMIC00139</sup>-*Gal4*; (Diao et al., 2015). The  
174 splicing trap reporter consists of a splice acceptor site and an in-frame *T2A-Gal4*  
175 sequence inserted in an intron between two coding exons. This *Gal4* cassette gets  
176 incorporated into *mbl* mRNA during splicing and therefore Gal4 is only present when  
177 *mbl* is translated. Consistent with previous studies, and its role in repressing the  
178 production of *Dscam2.10A*, all four *mbl* reporters were expressed in the third instar  
179 photoreceptors (Fig 3A, S3A-S3B and data not shown). We next did a more  
180 extensive characterization of *mbl* expression by driving nuclear localized GFP  
181 (*GFP.nls*) with one transcriptional (*mbl*<sup>NP0420</sup>-*Gal4*) and one translational  
182 (*mbl*<sup>MiMIC00139</sup>-*Gal4*) reporter. In the brain, we found that *mbl* was expressed  
183 predominantly in postmitotic neurons with some expression detected in glial cells (Fig  
184 S3C-S3F and S3H-S3K). Interestingly, we detected the translational but not the  
185 transcriptional reporter in third instar muscles (Fig S3G and S3L). The absence of  
186 expression is likely due to the insertion of the *P*-element into a neural-specific  
187 enhancer, as previously described (Bargiela et al., 2014). To assess the expression of  
188 *mbl* in the five lamina neurons L1- L5, all of which express *Dscam2* (Lah et al., 2014;  
189 Tadros et al., 2016), we implemented an intersectional strategy using a  
190 *UAS>stop>epitope* reporter (Nern et al., 2015) that is dependent on both *FLP* and  
191 *Gal4*. The *FLP* source (*Dac-FLP*) was expressed in lamina neurons and able to  
192 remove the transcriptional stop motif in the reporter transgene. The overlap between  
193 *mbl-Gal4* and *Dac-FLP* allowed us to visualize *mbl* expression in lamina neurons at  
194 single-cell resolution (Fig 3B). As a proof of principle, we first did an intersectional  
195 analysis with a pan-neuronal reporter, *elav-Gal4* (Fig 3C<sub>1</sub>). We detected many clones  
196 encompassing various neuronal-cell-types including the axons of L1-L5 and R7-R8

197 (Fig 3C-3D). This confirmed that all lamina neurons could be detected using this  
198 strategy. Using *mbl-Gal4* reporters we found that L1, which expresses *Dscam2.10B*,  
199 was the primary neuron labelled. A few L4 cells were also identified, which is  
200 consistent with this neuron expressing *Dscam2.10B* early in development and  
201 *Dscam2.10A* at later stages (Tadros et al., 2016). To confirm this finding, we  
202 dissected the expression of *mbl* in lamina neurons during development. Using the  
203 same intersectional strategy, we detected a high number of L4 clones at 48hr apf  
204 (30%, n=10). This was followed by a decline at 60hr apf (26.7%, n = 30) and 72hr apf  
205 (11.8%, n = 85) reaching the lowest at eclosion (Fig S4A and S4B; 1.7%, n=242).  
206 Thus, *mbl* expression in L4 neurons mirrors the expression of *Dscam2.10B*.  
207 Consistent with this, L2, L3 and L5, were all detected using the intersectional strategy  
208 with *Dscam2.10A-Gal4* but were not labelled using *mbl-Gal4* (Fig 3E). Together,  
209 these results show that cell-type-specific *mbl* expression is transcriptionally regulated  
210 and correlates with the cell-type-specific alternative splicing of *Dscam2*. Cells that  
211 select *Dscam2.10B* and repress *Dscam2.10A* express *mbl*. In contrast, *mbl* was not  
212 detected in cells that repress *Dscam2.10B* and select *Dscam2.10A*.

213

#### 214 **Ectopic expression of multiple *mbl* isoforms are sufficient to promote the** 215 **selection of *Dscam2* exon 10B**

216 Our analysis in the visual system demonstrated that *mbl* is necessary for the selection  
217 of *Dscam2.10B*, but we wondered whether it was sufficient to promote exon 10B  
218 selection in cell types that normally repress this isoform. To test this possibility, we  
219 overexpressed *mbl* ubiquitously and monitored isoform B expression using  
220 *Dscam2.10B>tdTom*. We focussed on the mushroom body (MB), as this tissue  
221 expresses isoform A specifically in  $\alpha'\beta'$  neurons at 24hr apf where *mbl* is not

222 detected (Fig 3G-3H, 4A-4C). Consistent with *mb1* being sufficient for isoform B  
223 selection, ubiquitous expression of *mb1* using an enhancer trap containing a *UAS*  
224 insertion at the 5' end of the gene (*Act5c>mb1<sup>B2-E1</sup>*), switched on *Dscam2.10B* in  $\alpha'\beta'$   
225 MB neurons, where it is normally absent (Fig 4D). Ectopic *mb1* expression in MB  
226 neurons with *OK107-Gal4* also led to selection of *Dscam2.10B* expression  
227 specifically in  $\alpha'\beta'$  neurons at 24-36hr apf. Although our two *Gal4* drivers expressed  
228 *mb1* in all MB neurons, *Dscam2.10B* was only observed in  $\alpha'\beta'$  neurons,  
229 demonstrating that transcription of *Dscam2* is a pre-requisite for this splicing  
230 modulation. Previous studies have suggested that the *mb1* gene is capable of  
231 generating different isoforms with unique functions depending on their subcellular  
232 localization (Vicente et al., 2007). This also includes the production of a highly  
233 abundant circular RNA that can sequester the Mbl protein (Ashwal-Fluss et al., 2014;  
234 Houseley et al., 2006). To assess whether *Dscam2* exon 10B selection is dependent on  
235 a specific alternative variant of Mbl, we overexpressed the cDNAs of fly *mb1*  
236 isoforms (*mb1A*, *mb1B* and *mb1C*; (Begemann et al., 1997; Juni and Yamamoto, 2009)  
237 as well as an isoform of the human *MBNL1* that lacks the linker region optimal for  
238 CUG repeat binding (*MBNL1<sub>35</sub>*; (Kino et al., 2004; Li et al., 2008) with either *Act5c-*  
239 *Gal4* or *OK107-Gal4*. These constructs all possess the tandem N-terminal CCCH  
240 motif that binds to YCGY sequences and lack the ability to produce *mb1* circRNA. In  
241 all cases, overexpression resulted in the misexpression of *Dscam2.10B* in  $\alpha'\beta'$  MBs  
242 (with the exception *Act5C>mb1C*, which resulted in lethality; Fig 4D-4E). Using  
243 semi-quantitative RT-PCR from the *Act5C>mb1* flies, we demonstrated that  
244 overexpression of *mb1* did not lead to exon 10 skipping and that it increased exon 10B  
245 selection by 8-24% (Fig 4F), depending on the *mb1* isoform used. The inability of Mbl  
246 to completely inhibit exon 10A selection suggests that other factors or mechanisms

247 may also contribute to cell-specific *Dscam2* isoform expression (see Discussion).  
248 These results suggest that Mbl protein isoforms are all capable of *Dscam2.10B*  
249 selection and independent of *mbl* circRNA. The ability of human MBNL1 to promote  
250 the selection of exon 10B suggests that the regulatory logic for *Dscam2* splicing is  
251 likely conserved in other mutually-exclusive cassettes in higher organisms.  
252  
253 Finally, we observed a phenotype in MB neurons overexpressing *mbl* where the  $\beta$   
254 lobe neurons inappropriately crossed the midline (Fig 4G-4I). Interestingly, a similar  
255 phenotype was observed in flies expressing a single isoform of *Dscam2* that we  
256 previously generated using recombinase-mediated cassette exchange (Lah et al.,  
257 2014). These flies express a single isoform in all *Dscam2* positive cells. We  
258 quantified this phenotype and found that the *Dscam2A*, but not the *Dscam2B*, single  
259 isoform line generated a MB fusion phenotype that was significantly different from  
260 controls. All of the *UAS-mbl* constructs, except human *MBNL1*, generated this  
261 phenotype at a penetrance that was equal to or greater than *Dscam2A* single isoform  
262 lines (Fig 4I). The lack of a phenotype with the human transgene is consistent with  
263 this modified isoform having a reduced CUG-binding capacity due to its missing  
264 linker domain (Kino et al., 2004; Li et al., 2008). These data demonstrate that MB  
265 phenotypes generated in animals overexpressing *mbl*, phenocopy *Dscam2* single  
266 isoform mutants. While the origin of this non-autonomous phenotype is not known, it  
267 correlates with the misregulation of *Dscam2* alternative isoform expression.

268

## 269 **Discussion**

270 In this study, we identify Mbl as a regulator of *Dscam2* alternative splicing. We  
271 demonstrate that removing *mbl* in a *mbl*-positive cell-type results in a switch from

272 *Dscam2.10B* to *Dscam2.10A* selection. Ectopic expression of a variety of Mbl protein  
273 isoforms in a normally *mbl*-negative neuronal cell-type is sufficient to trigger the  
274 selection of *Dscam2.10B*. Consistent with this, transcriptional reporters demonstrate  
275 that *mbl* is expressed in a cell-type-specific manner, which tightly correlates with  
276 *Dscam2.10B*. Lastly, misexpression of *mbl* leads to a MB phenotype that is also  
277 observed in flies that express a single *Dscam2* isoform.

278

279 One surprising finding in this study was that *mbl* expression itself is regulated in a  
280 cell-specific manner. *Mbl* was present in all cells tested that express *Dscam2.10B* and  
281 absent from *Dscam2.10A* cells. Mbl appears to be regulated at the transcriptional level  
282 since enhancer-trap as well as splicing-trap reporters exhibit similar expression  
283 patterns (Fig 3). This was unexpected as 1) examples of cell-specific expression of  
284 splicing factors are rare in the literature and 2) *mbl* encodes numerous alternative  
285 isoforms that could be individually post-transcriptionally regulated, thus bypassing  
286 the need for transcriptional control of the gene. It will be interesting to explore the *in*  
287 *vivo* expression patterns of other splicing factors to determine whether cell-specific  
288 expression of a subset of splicing factors is a common mechanism for regulating  
289 alternative splicing in the brain.

290

291 Given that Mbl can repress exon 10A and select exon 10B (Fig 4J), it is possible that  
292 this single splicing factor and its associated co-factors are sufficient to regulate  
293 *Dscam2* cell-specific isoform expression. It could be that *Dscam2.10A* is the default  
294 exon selected when the Mbl complex is not present. In this way, cells that express  
295 *Dscam2* would be ‘10A’ positive if they did not express *mbl* and ‘10B’ positive if  
296 they did. The observation that *Dscam2* is not expressed in all neurons and our RT-



297 PCR data, however, argue that *Dscam2* mutually exclusive alternative splicing may  
298 be more complicated than this model. In MB  $\alpha'\beta'$  neurons, which select exon 10A,  
299 ectopic expression of *mbl* using *Act5C-Gal4* can switch on a *Dscam2.10B>tdTom*  
300 reporter, but the change in isoform expression in the whole brain as measured by RT-  
301 PCR is only 8-24% (see Fig 4F). One might expect a much more dramatic shift to  
302 isoform B if *Mbl* were the only regulator/mechanism involved. In addition, if  
303 *Dscam2.10A* were expressed by default in the absence of *mbl*, we would expect all  
304 MB neurons to express this isoform, but this is not the case. Further studies, including  
305 screens for repressors or activators of exon 10B, will be required to resolve this issue.  
306  
307 The MB midline crossing phenotype that is generated through both the ectopic  
308 expression of *mbl* and *Dscam2A* single isoform lines supports the idea that this  
309 phenotype arises from a disruption in *Dscam2* cell-specific isoform expression.  
310 However, since both single isoform lines have identical expression patterns  
311 (expressed in all *Dscam2*-positive cells), one would expect both lines to exhibit the  
312 midline crossing phenotype if it is caused by inappropriate homophilic interactions  
313 between cells that normally express different isoforms. Although there is a trend  
314 towards increased fusion in animals expressing only *Dscam2B* (Fig 4I), it did not  
315 reach statistical significance. This issue may have to do with innate differences  
316 between isoform A and isoform B that are not completely understood. It is possible  
317 that isoform A and B are not identical in terms of signalling due to either differences  
318 in homophilic binding or differences in co-factors associated with specific isoforms.  
319 Consistent with this notion, we previously reported that *Dscam2A* lines produce  
320 stronger phenotypes at photoreceptor synapses compared to *Dscam2B*. Another  
321 perplexing aspect about the MB phenotype is that it occurs in neurons that either do

322 not express *Dscam2* ( $\beta$  lobe neurons) or express it at such low levels that it is not  
323 detectable with our reporters. Thus, the phenotype must arise indirectly. This could  
324 occur through inappropriate interactions between  $\alpha'$  $\beta'$  neurons and another non-MB  
325 cell type within this brain region that expresses *Dscam2*. Alternatively, this phenotype  
326 could be independent of *Dscam2* homophilic binding and instead reflect differences in  
327 isoform complexes that form in different neurons.

328

329 How does Mbl repress *Dscam2.10A* and select *Dscam2.10B* at the level of pre-  
330 mRNA? The vertebrate orthologue of Mbl, MBNL1 binds to YCGY (where Y is a  
331 pyrimidine) in pre-mRNAs and untranslated regions using its tandem zinc-finger  
332 domains, but it is quite promiscuous (Wang et al., 2012). The best-characterised  
333 alternative splicing events regulated by MBNL1 are exon skipping or inclusion  
334 events. In general, an exon that contains MBNL1 binding sites upstream or within the  
335 coding sequence is subject to skipping, whereas downstream binding sites more often  
336 promote inclusion (reviewed in Konieczny et al 2014). The mechanisms used by fly  
337 Mbl to regulate splicing have not been characterised in detail, but given that human  
338 MBNL1 can rescue fly *mbl* lethality and promote the endogenous expression of  
339 *Dscam2* exon 10B in MBs, presumably the mechanisms are conserved. A simple  
340 explanation for how Mbl regulates *Dscam2* mutually exclusive splicing would be that  
341 it binds upstream of exon 10A to repress exon inclusion and downstream of exon 10B  
342 to promote inclusion. Although there are many potential binding sites for Mbl  
343 upstream, downstream and within the alternative exons, an obvious correlation  
344 between location and repression vs inclusion is not observed. There is also a large  
345 (3kb) intron downstream of exon 10B that could contain *cis* regulatory elements.  
346 Identification of the sequences required for regulation by Mbl will therefore require

347 extensive mapping and ultimately validation using a technique like cross-linking  
348 followed by immunoprecipitation (CLIP).  
349  
350 Together, our results demonstrate that selective expression of a splicing factor can  
351 drive neuronal cell-type specific alternative splicing. These data provide clues into  
352 how the brain can diversify its repertoire of proteins that promote neural connectivity.  
353 It is likely that Mbl is regulating the alternative splicing of other developmental genes  
354 in concert with *Dscam2* and therefore regulated splicing factors such as Mbl may  
355 represent hubs of neurodevelopment.

356

## 357 **Experimental procedures**

### 358 **Fly strains**

359 *Dscam2.10A-LexA* and *Dscam2.10B-LexA* (Tadros et al., 2016), *UAS-Dcr2* and *UAS-*  
360 *mbl-RNAi<sup>VDRC28732</sup>* (Dietzl et al., 2007), *LexAop-myr-tdTomato* (attP2, (Chen et al.,  
361 2014), *UAS-Srp54-RNAi<sup>TRiP.HMS03941</sup>*, *CadN-RNAi<sup>TRiP.HMS02380</sup>* and *UAS-mbl-*  
362 *RNAi<sup>TRiP.JF03264</sup>* (Ni et al., 2008), *UAS-mCD8-GFP* (Lee and Luo, 1999), *FRT42D* (Xu  
363 and Rubin, 1993), *mbl<sup>e127</sup>* and *mbl<sup>e27</sup>* (Begemann et al., 1997), *mbl<sup>MI00976</sup>* and *mbl<sup>MI04093</sup>*  
364 (Venken et al., 2011), *Df(2R)BSC154* (Cook et al., 2012), *Df(2R)Exel6066* (Parks et  
365 al., 2004), *ey-FLP* (Chr.1, (Newsome et al., 2000), *GMR-myr-GFP*, *mbl<sup>NP0420</sup>-Gal4*  
366 and *mbl<sup>NP1161</sup>-Gal4* (Hayashi et al., 2002), *mbl<sup>k01212</sup>-LacZ* (Spradling et al., 1999),  
367 *mbl<sup>MiMIC00139</sup>-Gal4* (H. Bellen Lab), *Dac-FLP* (Chr.3, (Millard et al., 2007),  
368 *UAS>stop>myr::smGdP-V5-THS-UAS>stop>myr::smGdP-cMyc* (attP5, (Nern et al.,  
369 2015), *Dscam2.10A-Gal4* and *Dscam2.10B-Gal4* (Lah et al., 2014) *Act5C-Gal4*  
370 (Chr.3, from Yash Hiromi), *OK107-Gal4* (Connolly et al., 1996), *UAS-mblA*, *UAS-*

371 *mbIB* and *UAS-mblC* (D. Yamamoto Lab), *P{EP}mbl<sup>B2-E1</sup>*, *UAS-mblA-FLAG* and  
372 *UAS-MBNLI<sub>35</sub>* (Li et al., 2008).

373

#### 374 **RNAi screening**

375 The RNAi screen line was generated as follows: *GMR-Gal4* was recombined with  
376 *GMR-GFP* on the second chromosome. *Dscam2.10A-LexA* (Tadros et al. 2016) was  
377 recombined with *LexAop-myr-tdTomato* on the third chromosome. These flies were  
378 crossed together with *UAS-Dcr-2* (X) to make a stable RNAi screen stock. Virgin  
379 females were collected from this RNAi screen stock, crossed to UAS-RNAi males  
380 and reared at 25°C. Wandering third instar larvae were dissected and fixed. We tested  
381 between one and three independent RNAi lines per gene. Brains were imaged without  
382 antibodies using confocal microscopy. RNAi lines tested are listed in Table S1.

383

#### 384 **Semiquantitative RT-PCR**

385 Total RNA was isolated using TRIzol (Ambion) following the manufacturer's  
386 protocol. Reverse transcription was performed on each RNA sample with random  
387 primer mix using 200 units of M-MULV (NEB) and 2  $\mu$  g of RNA in a 20  $\mu$  l  
388 reaction, at 42°C for 1 hr. PCR reactions were set up with specific primers to analyse  
389 alternative splicing of various regions of *Dscam2*. Where possible, semi-quantitative  
390 PCR was performed to generate multiple isoforms in a single reaction and relative  
391 levels were compared by electrophoresis.

392

#### 393 **Immunohistochemistry**

394 Immunostaining were conducted as previously described (Lah et al. 2014). Antibody  
395 dilutions used were as follows: mouse mAb24B10 (1:20; DSHB), mouse anti-Repo

396 (1:20; DSHB), mouse anti-DAC (1:20; DSHB), mouse anti-Fas2 (1:20; DSHB) rat  
397 anti-ELAV (1:200), V5-tag:DyLight anti-mouse 550 (1:500; AbD Serotec), V5-  
398 tag:DyLight anti-mouse 405 (1:200; AbD Serotec), myc-tag:DyLight anti-mouse 549  
399 (1:200; AbD Serotec), Phalloidin:Alexa Fluor 568 (1:200; Molecular Probes),  
400 DyLight anti-mouse 647 (1:2000; Jackson Laboratory), DyLight Cy3 anti-rat (1:2000;  
401 Jackson Laboratory).

402

### 403 **Image acquisition**

404 Imaging was performed at the School of Biomedical Sciences Imaging Facility.  
405 Images were taken on a Leica SP8 laser scanning confocal system with a 63X  
406 Glycerol NA 1.3.

407

### 408 **Fly genotypes**

#### 409 R cell RNAi experiments (Figure 1)

410 *w; GMR-GFP, GMR-Gal4/CyO; Dscam2.10B-LexA, LexAop-myr-tdTomato/TM6B*

411 *w; GMR-GFP, GMR-Gal4/CyO; Dscam2.10A-LexA, LexAop-myr-tdTomato/TM6B*

412 *w, UAS-Dcr-2; GMR-GFP, GMR-Gal4/CyO; Dscam2.10A-LexA, LexAop-myr-*

413 *tdTomato/TM6B*

414 *w, UAS-Dcr-2; GMR-GFP, GMR-Gal4/UAS-mCD8-RFP; Dscam2.10A-LexA,*

415 *LexAop-myr-tdTomato/+*

416 *w, UAS-Dcr-2; GMR-GFP, GMR-Gal4/UAS-mbl-RNAi(v28732); Dscam2.10A-LexA,*

417 *LexAop-myr-tdTomato/+*

418 *w, UAS-Dcr-2; GMR-GFP, GMR-Gal4/+; Dscam2.10A-LexA, LexAop-myr-*

419 *tdTomato/UAS-mbl-RNAi(TRiP.JF03264)*

420

- 421 mbl whole animal experiments (Figure 1)
- 422 *w; +; Dscam2.10B-LexA, LexAop-myr-tdTomato/TM6B*
- 423 *w; +; Dscam2.10A-LexA, LexAop-myr-tdTomato/TM6B*
- 424 *w; mbl<sup>e127</sup>/CyO,GFP; Dscam2.10A-LexA, LexAop-myr-tdTomato/TM6B*
- 425 *w; mbl<sup>M100976</sup>/CyO,GFP; Dscam2.10A-LexA, LexAop-myr-tdTomato/TM6B*
- 426 *w; mbl<sup>M104093</sup>/CyO,GFP; Dscam2.10A-LexA, LexAop-myr-tdTomato/TM6B*
- 427 *w; mbl<sup>e127</sup>/ mbl<sup>M100976</sup>; Dscam2.10A-LexA, LexAop-myr-tdTomato/+*
- 428 *w; mbl<sup>M104093</sup>/ mbl<sup>M100976</sup>; Dscam2.10A-LexA, LexAop-myr-tdTomato/+*
- 429
- 430 mbl ey-FLP mosaic experiments (Figure 1)
- 431 *w, ey-FLP; FRT42D, GMR-myr-GFP/FRT42D; Dscam2.10B-LexA, LexAop-myr-*
- 432 *tdTomato, UAS-mCD8-GFP/+*
- 433 *w, ey-FLP; FRT42D, GMR-myr-GFP/FRT42D; Dscam2.10A-LexA, LexAop-myr-*
- 434 *tdTomato, UAS-mCD8-GFP/+*
- 435 *w, ey-FLP; FRT42D, GMR-myr-GFP/FRT42D, Df(2R)154 ; Dscam2.10A-LexA,*
- 436 *LexAop-myr-tdTomato, UAS-mCD8-GFP/+*
- 437 *w, ey-FLP; FRT42D, GMR-myr-GFP/FRT42D, mbl<sup>e27</sup>; Dscam2.10A-LexA, LexAop-*
- 438 *myr-tdTomato, UAS-mCD8-GFP/+*
- 439 *w, ey-FLP; FRT42D, GMR-myr-GFP/FRT42D, mbl<sup>M100976</sup>; Dscam2.10A-LexA,*
- 440 *LexAop-myr-tdTomato, UAS-mCD8-GFP/+*
- 441
- 442 mbl ey-FLP MARCM experiments (Figure 3)
- 443 *w, ey-FLP; FRT42D, Tub-Gal80/FRT42D; Dscam2.10A-LexA, LexAop-myr-*
- 444 *tdTomato, Act5c-Gal4, UAS-mCD8-GFP/+*

445 *w, ey-FLP; FRT42D, Tub-Gal80/FRT42D, mbl<sup>e27</sup>; Dscam2.10A-LexA, LexAop-myr-*

446 *tdTomato, Act5c-Gal4, UAS-mCD8-GFP/+*

447 *w, ey-FLP; FRT42D, Tub-Gal80/FRT42D, mbl<sup>e127</sup>; Dscam2.10A-LexA, LexAop-myr-*

448 *tdTomato, Act5c-Gal4, UAS-mCD8-GFP/+*

449

450 *mbl* expression experiments (Figure 3)

451 *w; UAS-mCD8-GFP/+; mbl<sup>NP0420</sup>-Gal4/+*

452 *w; UAS-mCD8-GFP/+; mbl<sup>MI00139</sup>-Gal4/+*

453 *w; Dac-FLP/+; elav-Gal4/ UAS>stop>myr::smGdP-V5-THS-*

454 *UAS>stop>myr::smGdP-cMyc*

455 *w; Dac-FLP/+; mbl<sup>NP0420</sup>-Gal4/ UAS>stop>myr::smGdP-V5-THS-*

456 *UAS>stop>myr::smGdP-cMyc*

457 *w; Dac-FLP/+; mbl<sup>MI00139</sup>-Gal4/ UAS>stop>myr::smGdP-V5-THS-*

458 *UAS>stop>myr::smGdP-cMyc*

459 *w; Dac-FLP/+; Dscam2.10A-Gal4/ UAS>stop>myr::smGdP-V5-THS-*

460 *UAS>stop>myr::smGdP-cMyc*

461 *w; Dac-FLP/+; Dscam2.10B-Gal4/ UAS>stop>myr::smGdP-V5-THS-*

462 *UAS>stop>myr::smGdP-cMyc*

463 *w; +; mbl<sup>NP0420</sup>-Gal4/UAS-GFP.nls*

464 *w; +; mbl<sup>MI00139</sup>-Gal4/UAS-GFP.nls*

465

466 *mbl* ectopic expression in MBs (Figure 4)

467 *w; +; Dscam2.10A-LexA, LexAop-myr-tdTomato, Act5c-Gal4, UAS-mCD8-GFP/+*

468 *w; +; Dscam2.10B-LexA, LexAop-myr-tdTomato, Act5c-Gal4, UAS-mCD8-GFP/+*

469 *w; P{EP}mbl<sup>B2-E1</sup>/+; Dscam2.10B-LexA, LexAop-myr-tdTomato, Act5c-Gal4, UAS-*  
470 *mCD8-GFP/+*  
471 *w; +; Dscam2.10B-LexA, LexAop-myr-tdTomato, Act5c-Gal4, UAS-mCD8-*  
472 *GFP/UAS-mblA*  
473 *w; +; Dscam2.10B-LexA, LexAop-myr-tdTomato, Act5c-Gal4, UAS-mCD8-*  
474 *GFP/UAS-mblB*  
475 *w; +; Dscam2.10B-LexA, LexAop-myr-tdTomato, Act5c-Gal4, UAS-mCD8-*  
476 *GFP/UAS-mblC*  
477 *w; +; Dscam2.10B-LexA, LexAop-myr-tdTomato, Act5c-Gal4, UAS-mCD8-GFP/UAS-*  
478 *MBNL1<sub>35</sub>*  
479 *w; +; Dscam2.10B-LexA, LexAop-myr-tdTomato, UAS-mCD8-GFP/UAS-mblA;*  
480 *OK107-Gal4/+*  
481 *w; +; Dscam2.10B-LexA, LexAop-myr-tdTomato, UAS-mCD8-GFP/UAS-mblB;*  
482 *OK107-Gal4/+*  
483 *w; +; Dscam2.10B-LexA, LexAop-myr-tdTomato, UAS-mCD8-GFP/UAS-mblC;*  
484 *OK107-Gal4/+*  
485 *w; +; Dscam2.10B-LexA, LexAop-myr-tdTomato, UAS-mCD8-GFP/UAS-MBNL1<sub>35</sub>;*  
486 *OK107-Gal4/+*

487  
488

#### 489 **Author contribution**

490 J.S.S.L designed and performed all experiments. S.S.M supervised the project. J.S.S.L  
491 and S.S.M wrote the manuscript.

492

#### 493 **Acknowledgements**



494 We thank Wael Tadros, Larry Zipursky, Greg Neely, Louis O’Keefe, Nancy Bonini,  
495 Aljoscha Nern and Bloomington Stock Center for sharing fly stocks. We thank the  
496 Daisuke Yamamoto Lab for constructing the *UAS-mbl* lines deposited and maintained  
497 at the Kyoto Stock Center. We thank Shaun Walters for technical assistance on the  
498 Leica confocal microscopy. We thank Kevin Mutemi for characterizing *Dscam2*  
499 isoform expression in mushroom bodies and all midline crossing defects in *Dscam2*  
500 single isoform mutant animals. We thank Grace Shin for her initial characterization of  
501 *Dscam2* isoform expression in adults and Wei Jun Tan for triple balancing *OK107-*  
502 *Gal4*. We also thank members of the Millard, Pecot, Hilliard and van Swinderen lab  
503 for their feedback. The RNAi screen was inspired by the works of Hidehito  
504 Kuroyanagi. This work was supported by the National Health and Medical Research  
505 Council of Australia (NHMRC grant APP1021006). J.S.S.L was supported by the  
506 Australia Postgraduate Award (Research Training Scheme) from the Australian  
507 Federal Government.

508

## 509 **Figure legends**

510 **Figure 1.** *Drosophila mbl* is required for the repression of *Dscam2* exon 10A in R  
511 cells. (A) Schematic showing the region of *Dscam2* exon 10 that undergoes mutually  
512 exclusive alternative splicing and the LexA isoform-specific reporter lines. Frame-  
513 shift mutations in the exon not reported are shown. (B) Schematic RNAi screen  
514 design for identifying repressors of *Dscam2* exon 10A selection. R cells normally  
515 select exon 10B and repress exon 10A. We knocked-down RNA binding proteins in R  
516 cells while monitoring 10A expression.  
517 (C-E) *Dscam2* exon 10A is derepressed in R cells when *mbl* is knocked-down. (C<sub>1</sub>-  
518 C<sub>3</sub>) *Dscam2.10B* control. R cells (green) normally select exon 10B (red). R cell

519 terminals can be observed in the lamina plexus (angle brackets). *Dscam2.10B* is also  
520 expressed in the developing optic lobe (arrowhead). (D<sub>1</sub>-D<sub>3</sub>) *Dscam2.10A* is not  
521 expressed in R cells (green) but is expressed in the developing optic lobe (arrowhead).  
522 (E<sub>1</sub>-E<sub>3</sub>) RNAi lines targeting *mbl* in R cells results in the aberrant expression of  
523 *Dscam2.10A* in R cells.

524 (F) Schematic of the *mbl* gene showing the location of two small deletions (*E27* and  
525 *E127*), two MiMIC insertions (*MI04093* and *MI00976*) and two deficiencies  
526 (*Df(2R)Exel6066* and *Df(2R)BSC154*) used in this study. Non-coding exons are in  
527 gray, coding exons are black.

528 (G) Complementation test of *mbl* loss-of-function (LOF) alleles. Numbers in the table  
529 represent the number of non-*CyO* offspring over the total. Most transheterozygote  
530 combinations were lethal with the exception of *mbl*<sup>MI00976</sup>/*mbl*<sup>e27</sup> and  
531 *mbl*<sup>MI00976</sup>/*mbl*<sup>MI04093</sup> (green).

532 (H-N) *Mbl* transheterozygotes express *Dscam2.10A* in R cells. (H) *Dscam2.10B*  
533 control showing expression in the lamina plexus (angle brackets). (I) *Dscam2.10A*  
534 control showing no expression of this isoform in R cells. (J-L) Heterozygous animals  
535 for *mbl* LOF alleles are comparable to control. (M-N) Two different *mbl*  
536 transheterozygote combinations exhibit de-repression of *Dscam2.10A* in R cells.

537 (O) Quantification of *Dscam2.10>tdTom* expression in third instar R cells with  
538 various *mbl* manipulations; including RNAi knockdown (black bars) and whole  
539 animal transheterozygotes (white). Y-axis represents the number of optic lobes with R  
540 cells positive for tdTom over total quantified as a percentage. On the x-axis, the  
541 presence of a transgene is indicated with a blue box and the temperature at which the  
542 crosses were reared (25°C or 29°C) is indicated.

543 (P) *Dscam2* exon 10A inclusion is increased in *mbl* transheterozygotes. (Top)  
544 Semiquantitative RT-PCR from different genotypes indicated. Primers amplified the  
545 variable region that includes exon 10. A smaller product that would result from exon  
546 10 skipping is not observed. (Bottom) Exon 10A-specific cleavage with restriction  
547 enzyme *Cl*I shows an increase in exon 10A inclusion in *mbl* transheterozygotes.  
548 Percentage of exon 10A inclusion was calculated by dividing 10A by 10A+10B bands  
549 following restriction digest. See also Figures S1 and S2.

550

551 **Figure 2.** *Drosophila* Mbl is necessary for the selection of *Dscam2* exon 10B in R  
552 cells.

553 (A) Schematic of our predicted *mbl* MARCM results using *ey-FLP*. WT R cell clones  
554 will be GFP(+) and *Dscam2.10B>tdTom*(+) (yellow), whereas *mbl* mutant clones will  
555 be *Dscam2.10B>tdTom*(-) (green). (B<sub>1</sub>-B<sub>3</sub>) Control MARCM clones (green) in 3<sup>rd</sup>  
556 instar R cells (angle brackets) are positive for *Dscam2.10B>tdTom* (arrowhead). (C<sub>1</sub>-  
557 C<sub>3</sub>) In *mbl<sup>e27</sup>* clones, *Dscam2.10B* labelling in the lamina plexus is discontinuous and  
558 its absence correlates with the loss of Mbl (arrowhead). (D<sub>1</sub>-D<sub>2</sub>) *Mbl* MARCM clones  
559 from midpupal optic lobes lack *Dscam2.10B>tdTom*. (E<sub>1</sub>-E<sub>3</sub>) A different allele  
560 (*mbl<sup>e127</sup>*) exhibits a similar phenotype in third instar brains.

561

562 **Figure 3.** *Mbl* is expressed in a cell-specific manner that correlates with

563 *Dscam2.10B*

564 (A) A *mbl* Gal4 reporter (green) is expressed in third instar R cells but not in lamina  
565 neuron precursor cells labelled with an antibody against Dacshund (DAC, red).

566 (B) Schematic of MultiColor FlpOut (MCFO) approach to characterize *mbl* reporter  
567 expression in lamina neurons at adult stages. The UAS FlpOut construct produces an  
568 epitope-tagged version of a non-fluorescent GFP (smGFP,(Nern et al., 2015))  
569 ( $C_1$ - $C_4$ ) *Mbl* can be detected in all lamina neurons using a MCFO strategy with a pan-  
570 neuronal reporter (*elav-Gal4*). Lamina neurons were identified based on their unique  
571 axon morphologies. ( $D_1$ - $D_4$ ) An intersectional strategy using *mbl-Gal4* labels  
572 primarily L1 lamina neurons. (E) Quantification of lamina neurons and R7-R8  
573 neurons observed using the intersectional strategy. Dark blue and light blue boxes  
574 represent high and low numbers of labelled neurons, respectively. (F-H) *Mbl* is not  
575 expressed in mushroom body (MB) neurons that express *Dscam2.10A* at 24hr apf.  
576 ( $F_1$ - $F_2$ ) *Dscam2.10A* is expressed in  $\alpha'\beta'$  MB neurons that are not labelled by Fas2.  
577 Fas2 labels the  $\alpha\beta$  and  $\gamma$  subsets of MB neurons. (G-H) Neither *Dscam2.10B* ( $G_1$ - $G_2$ )  
578 nor *mbl* ( $H_1$ - $H_2$ ) are detected in MB neurons. See also Figures S3 and S4.

579

580 **Figure 4.** All fly *mbl* isoforms can select *Dscam2* exon 10B and promote a midline  
581 crossing phenotype in MBs.

582 (A) Schematic showing that *mbl* is sufficient to drive *Dscam2.10B* selection in  
583  $\alpha'\beta'$  neurons.

584 (B) Control showing that *Dscam2.10A* (red) is expressed in  $\alpha'\beta'$  neurons at 24hr apf.

585 (C) *Dscam2.10B* is normally repressed in  $\alpha'\beta'$  neurons. (D) Overexpression of *mbl*  
586 activates *Dscam2.10B* selection (red) in  $\alpha'\beta'$  neurons. (E) Quantification of

587 *Dscam2.10* expression in  $\alpha'\beta'$  neurons at 24-36hr apf with and without *mbl* OE.

588 Ubiquitous driver (*Act5c-Gal4*, black bars) and pan-mushroom body neuron driver

589 (*OK107-Gal4*, white bars). Y-axis represents the number of tdTom positive (+)  $\alpha'\beta'$

590 over the total, expressed as a percentage. Ratio of tdTom(+)/total is shown in each

591 bar. (F) *Mbl* OE increases *Dscam2* exon 10B inclusion. Semiquantitative RT-PCR as  
592 in Figure 1. Exon 10A-specific cleavage with restriction enzyme *ClaI* shows an  
593 increase in exon 10B inclusion in *mbl* OE animals, without exon 10 skipping.  
594 (G) A representative confocal image of control adult  $\alpha\beta$  lobes (red) with clear  
595 separation between the two  $\beta$ -lobes at the midline. (H) A representative confocal  
596 image of adult  $\alpha\beta$  lobes from an animal overexpressing *mblA*.  $\beta$ -lobe axons  
597 inappropriately cross the midline (arrowhead). (I) Quantification of  $\beta$ -lobe axon  
598 midline crossing defects. Numbers in parentheses represent total number of  
599 mushroom bodies quantified. Fishers exact test was used to compare genotypes to  
600 their corresponding controls (white bars). n.s (not significant)  $P>0.05$ , \*  $P<0.05$  and  
601 \*\*\*\*\*  $P<0.0001$ . (J) Model illustrating that *Mbl* represses *Dscam2.10A* and selects  
602 *Dscam2.10B*.

603  
604  
605  
606

607 **References**

- 608 Artero, R., Prokop, A., Paricio, N., Begemann, G., Pueyo, I., Mlodzik, M., Perez-  
609 Alonso, M., and Baylies, M.K. (1998). The muscleblind gene participates in the  
610 organization of Z-bands and epidermal attachments of *Drosophila* muscles and is  
611 regulated by Dmef2. *Developmental biology* 195, 131-143.
- 612 Ashwal-Fluss, R., Meyer, M., Pamudurti, N.R., Ivanov, A., Bartok, O., Hanan, M.,  
613 Evantal, N., Memczak, S., Rajewsky, N., and Kadener, S. (2014). circRNA  
614 biogenesis competes with pre-mRNA splicing. *Molecular cell* 56, 55-66.
- 615 Bargiela, A., Llamusi, B., Cerro-Herreros, E., and Artero, R. (2014). Two enhancers  
616 control transcription of *Drosophila* muscleblind in the embryonic somatic  
617 musculature and in the central nervous system. *PloS one* 9, e93125.
- 618 Begemann, G., Paricio, N., Artero, R., Kiss, I., Perez-Alonso, M., and Mlodzik, M.  
619 (1997). muscleblind, a gene required for photoreceptor differentiation in  
620 *Drosophila*, encodes novel nuclear Cys3His-type zinc-finger-containing proteins.  
621 *Development* 124, 4321-4331.
- 622 Bell, T.J., Thaler, C., Castiglioni, A.J., Helton, T.D., and Lipscombe, D. (2004). Cell-  
623 specific alternative splicing increases calcium channel current density in the pain  
624 pathway. *Neuron* 41, 127-138.
- 625 Blanchette, M., Green, R.E., MacArthur, S., Brooks, A.N., Brenner, S.E., Eisen, M.B.,  
626 and Rio, D.C. (2009). Genome-wide analysis of alternative pre-mRNA splicing and  
627 RNA-binding specificities of the *Drosophila* hnRNP A/B family members.  
628 *Molecular cell* 33, 438-449.
- 629 Brand, A.H., and Perrimon, N. (1993). Targeted gene expression as a means of  
630 altering cell fates and generating dominant phenotypes. *Development* 118, 401-  
631 415.
- 632 Brouwer, J., Nagelkerke, D., den Heijer, P., Ruiters, J.H., Mulder, H., Begemann, M.J.,  
633 and Lie, K.I. (1997). Analysis of atrial sensed far-field ventricular signals: a  
634 reassessment. *Pacing and clinical electrophysiology : PACE* 20, 916-922.
- 635 Calarco, J.A., Superina, S., O'Hanlon, D., Gabut, M., Raj, B., Pan, Q., Skalska, U.,  
636 Clarke, L., Gelinas, D., van der Kooy, D., *et al.* (2009). Regulation of vertebrate  
637 nervous system alternative splicing and development by an SR-related protein.  
638 *Cell* 138, 898-910.
- 639 Chen, Y., Akin, O., Nern, A., Tsui, C.Y., Pecot, M.Y., and Zipursky, S.L. (2014). Cell-  
640 type-specific labeling of synapses in vivo through synaptic tagging with  
641 recombination. *Neuron* 81, 280-293.
- 642 Connolly, J.B., Roberts, I.J., Armstrong, J.D., Kaiser, K., Forte, M., Tully, T., and  
643 O'Kane, C.J. (1996). Associative learning disrupted by impaired Gs signaling in  
644 *Drosophila* mushroom bodies. *Science* 274, 2104-2107.
- 645 Cook, R.K., Christensen, S.J., Deal, J.A., Coburn, R.A., Deal, M.E., Gresens, J.M.,  
646 Kaufman, T.C., and Cook, K.R. (2012). The generation of chromosomal deletions  
647 to provide extensive coverage and subdivision of the *Drosophila melanogaster*  
648 genome. *Genome biology* 13, R21.
- 649 Diao, F., Ironfield, H., Luan, H., Diao, F., Shropshire, W.C., Ewer, J., Marr, E., Potter,  
650 C.J., Landgraf, M., and White, B.H. (2015). Plug-and-play genetic access to  
651 *drosophila* cell types using exchangeable exon cassettes. *Cell reports* 10, 1410-  
652 1421.
- 653 Dietzl, G., Chen, D., Schnorrer, F., Su, K.C., Barinova, Y., Fellner, M., Gasser, B.,  
654 Kinsey, K., Oettel, S., Scheiblauer, S., *et al.* (2007). A genome-wide transgenic

655 RNAi library for conditional gene inactivation in *Drosophila*. *Nature* 448, 151-  
656 U151.

657 Hayashi, S., Ito, K., Sado, Y., Taniguchi, M., Akimoto, A., Takeuchi, H., Aigaki, T.,  
658 Matsuzaki, F., Nakagoshi, H., Tanimura, T., *et al.* (2002). GETDB, a database  
659 compiling expression patterns and molecular locations of a collection of Gal4  
660 enhancer traps. *Genesis* 34, 58-61.

661 Houseley, J.M., Garcia-Casado, Z., Pascual, M., Paricio, N., O'Dell, K.M., Monckton,  
662 D.G., and Artero, R.D. (2006). Noncanonical RNAs from transcripts of the  
663 *Drosophila* muscleblind gene. *The Journal of heredity* 97, 253-260.

664 Iijima, T., Iijima, Y., Witte, H., and Scheiffele, P. (2014). Neuronal cell type-specific  
665 alternative splicing is regulated by the KH domain protein SLM1. *The Journal of*  
666 *cell biology* 204, 331-342.

667 Irion, U. (2012). *Drosophila* muscleblind codes for proteins with one and two  
668 tandem zinc finger motifs. *PloS one* 7, e34248.

669 Juni, N., and Yamamoto, D. (2009). Genetic analysis of chaste, a new mutation of  
670 *Drosophila melanogaster* characterized by extremely low female sexual  
671 receptivity. *Journal of neurogenetics* 23, 329-340.

672 Kania, A., Salzberg, A., Bhat, M., D'Evelyn, D., He, Y., Kiss, I., and Bellen, H.J. (1995).  
673 P-element mutations affecting embryonic peripheral nervous system  
674 development in *Drosophila melanogaster*. *Genetics* 139, 1663-1678.

675 Kerwin, S.K., Li, J.S.S., Noakes, P.G., Shin, G.J., and Millard, S.S. (2018). Regulated  
676 Alternative Splicing of *Drosophila* Dscam2 Is Necessary for Attaining the  
677 Appropriate Number of Photoreceptor Synapses. *Genetics* 208, 717-728.

678 Kino, Y., Mori, D., Oma, Y., Takeshita, Y., Sasagawa, N., and Ishiura, S. (2004).  
679 Muscleblind protein, MBNL1/EXP, binds specifically to CHHG repeats. *Human*  
680 *molecular genetics* 13, 495-507.

681 Kuroyanagi, H., Kobayashi, T., Mitani, S., and Hagiwara, M. (2006). Transgenic  
682 alternative-splicing reporters reveal tissue-specific expression profiles and  
683 regulation mechanisms in vivo. *Nature methods* 3, 909-915.

684 Lah, G.J., Li, J.S., and Millard, S.S. (2014). Cell-specific alternative splicing of  
685 *Drosophila* Dscam2 is crucial for proper neuronal wiring. *Neuron* 83, 1376-1388.

686 Lai, S.L., and Lee, T. (2006). Genetic mosaic with dual binary transcriptional  
687 systems in *Drosophila*. *Nature neuroscience* 9, 703-709.

688 Lee, T., and Luo, L. (1999). Mosaic analysis with a repressible cell marker for  
689 studies of gene function in neuronal morphogenesis. *Neuron* 22, 451-461.

690 Li, J.S., Shin, G.J., and Millard, S.S. (2015). Neuronal cell-type-specific alternative  
691 splicing: A mechanism for specifying connections in the brain? *Neurogenesis* 2,  
692 e1122699.

693 Li, L.B., Yu, Z., Teng, X., and Bonini, N.M. (2008). RNA toxicity is a component of  
694 ataxin-3 degeneration in *Drosophila*. *Nature* 453, 1107-1111.

695 Llamusi, B., Bargiela, A., Fernandez-Costa, J.M., Garcia-Lopez, A., Klima, R.,  
696 Feiguin, F., and Artero, R. (2013). Muscleblind, BSF and TBPH are mislocalized in  
697 the muscle sarcomere of a *Drosophila* myotonic dystrophy model. *Disease*  
698 *models & mechanisms* 6, 184-196.

699 Markovtsov, V., Nikolic, J.M., Goldman, J.A., Turck, C.W., Chou, M.Y., and Black, D.L.  
700 (2000). Cooperative assembly of an hnRNP complex induced by a tissue-specific  
701 homolog of polypyrimidine tract binding protein. *Molecular and cellular biology*  
702 20, 7463-7479.



703 Millard, S.S., Flanagan, J.J., Pappu, K.S., Wu, W., and Zipursky, S.L. (2007). Dscam2  
704 mediates axonal tiling in the Drosophila visual system. *Nature* 447, 720-724.  
705 Millard, S.S., Lu, Z., Zipursky, S.L., and Meinertzhagen, I.A. (2010). Drosophila  
706 dscam proteins regulate postsynaptic specificity at multiple-contact synapses.  
707 *Neuron* 67, 761-768.  
708 Mondal, K., VijayRaghavan, K., and Varadarajan, R. (2007). Design and utility of  
709 temperature-sensitive Gal4 mutants for conditional gene expression in  
710 Drosophila. *Fly* 1, 282-286.  
711 Nern, A., Pfeiffer, B.D., and Rubin, G.M. (2015). Optimized tools for multicolor  
712 stochastic labeling reveal diverse stereotyped cell arrangements in the fly visual  
713 system. *Proceedings of the National Academy of Sciences of the United States of*  
714 *America* 112, E2967-E2976.  
715 Newsome, T.P., Schmidt, S., Dietzl, G., Keleman, K., Asling, B., Debant, A., and  
716 Dickson, B.J. (2000). Trio combines with dock to regulate Pak activity during  
717 photoreceptor axon pathfinding in Drosophila. *Cell* 101, 283-294.  
718 Ni, J.Q., Markstein, M., Binari, R., Pfeiffer, B., Liu, L.P., Villalta, C., Booker, M.,  
719 Perkins, L., and Perrimon, N. (2008). Vector and parameters for targeted  
720 transgenic RNA interference in Drosophila melanogaster. *Nature methods* 5, 49-  
721 51.  
722 Nilsen, T.W., and Graveley, B.R. (2010). Expansion of the eukaryotic proteome by  
723 alternative splicing. *Nature* 463, 457-463.  
724 Norris, A.D., Gao, S., Norris, M.L., Ray, D., Ramani, A.K., Fraser, A.G., Morris, Q.,  
725 Hughes, T.R., Zhen, M., and Calarco, J.A. (2014). A pair of RNA-binding proteins  
726 controls networks of splicing events contributing to specialization of neural cell  
727 types. *Molecular cell* 54, 946-959.  
728 Ohno, G., Hagiwara, M., and Kuroyanagi, H. (2008). STAR family RNA-binding  
729 protein ASD-2 regulates developmental switching of mutually exclusive  
730 alternative splicing in vivo. *Genes & development* 22, 360-374.  
731 Pan, Q., Shai, O., Lee, L.J., Frey, B.J., and Blencowe, B.J. (2008). Deep surveying of  
732 alternative splicing complexity in the human transcriptome by high-throughput  
733 sequencing. *Nature genetics* 40, 1413-1415.  
734 Parks, A.L., Cook, K.R., Belvin, M., Dompe, N.A., Fawcett, R., Huppert, K., Tan, L.R.,  
735 Winter, C.G., Bogart, K.P., Deal, J.E., *et al.* (2004). Systematic generation of high-  
736 resolution deletion coverage of the Drosophila melanogaster genome. *Nature*  
737 *genetics* 36, 288-292.  
738 Pascual, M., Vicente, M., Monferrer, L., and Artero, R. (2006). The Muscleblind  
739 family of proteins: an emerging class of regulators of developmentally  
740 programmed alternative splicing. *Differentiation; research in biological diversity*  
741 74, 65-80.  
742 Schreiner, D., Nguyen, T.M., Russo, G., Heber, S., Patrignani, A., Ahrne, E., and  
743 Scheiffele, P. (2014). Targeted combinatorial alternative splicing generates brain  
744 region-specific repertoires of neurexins. *Neuron* 84, 386-398.  
745 Spradling, A.C., Stern, D., Beaton, A., Rhem, E.J., Laverly, T., Mozden, N., Misra, S.,  
746 and Rubin, G.M. (1999). The Berkeley Drosophila Genome Project gene  
747 disruption project: Single P-element insertions mutating 25% of vital Drosophila  
748 genes. *Genetics* 153, 135-177.  
749 Tadros, W., Xu, S.W., Akin, O., Yi, C.H., Shin, G.J.E., Millard, S.S., and Zipursky, S.L.  
750 (2016). Dscam Proteins Direct Dendritic Targeting through Adhesion. *Neuron*  
751 89, 480-493.



752 Tomioka, M., Naito, Y., Kuroyanagi, H., and Iino, Y. (2016). Splicing factors control  
753 *C. elegans* behavioural learning in a single neuron by producing DAF-2c receptor.  
754 *Nature communications* 7, 11645.

755 Underwood, J.G., Boutz, P.L., Dougherty, J.D., Stoilov, P., and Black, D.L. (2005).  
756 Homologues of the *Caenorhabditis elegans* Fox-1 protein are neuronal splicing  
757 regulators in mammals. *Molecular and cellular biology* 25, 10005-10016.

758 Venken, K.J., Schulze, K.L., Haelterman, N.A., Pan, H., He, Y., Evans-Holm, M.,  
759 Carlson, J.W., Levis, R.W., Spradling, A.C., Hoskins, R.A., and Bellen, H.J. (2011).  
760 MiMIC: a highly versatile transposon insertion resource for engineering  
761 *Drosophila melanogaster* genes. *Nature methods* 8, 737-743.

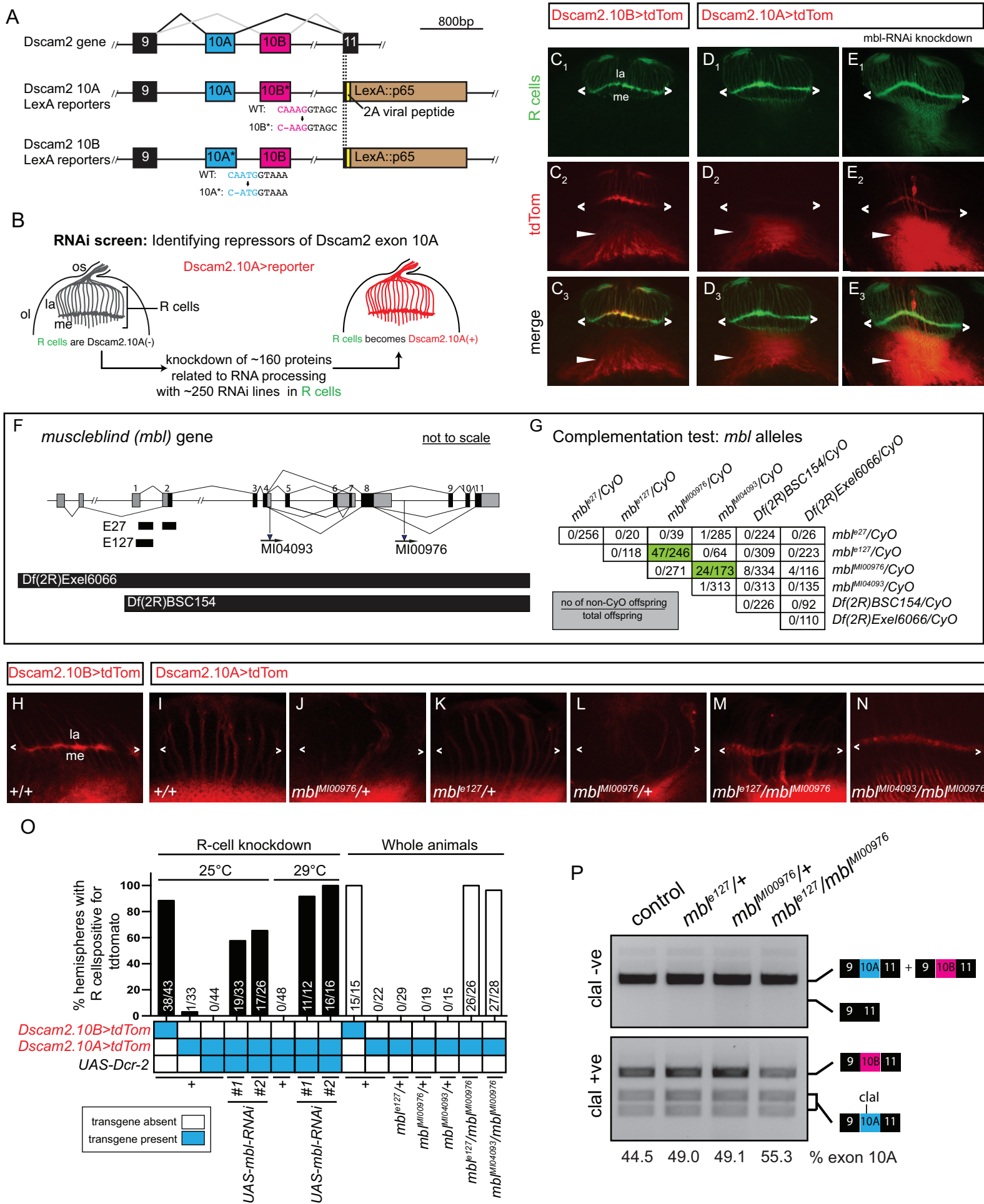
762 Vicente, M., Monferrer, L., Poulos, M.G., Houseley, J., Monckton, D.G., O'Dell K, M.,  
763 Swanson, M.S., and Artero, R.D. (2007). Muscleblind isoforms are functionally  
764 distinct and regulate alpha-actinin splicing. *Differentiation; research in biological*  
765 *diversity* 75, 427-440.

766 Wang, E.T., Cody, N.A., Jog, S., Biancolella, M., Wang, T.T., Treacy, D.J., Luo, S.,  
767 Schroth, G.P., Housman, D.E., Reddy, S., *et al.* (2012). Transcriptome-wide  
768 regulation of pre-mRNA splicing and mRNA localization by muscleblind proteins.  
769 *Cell* 150, 710-724.

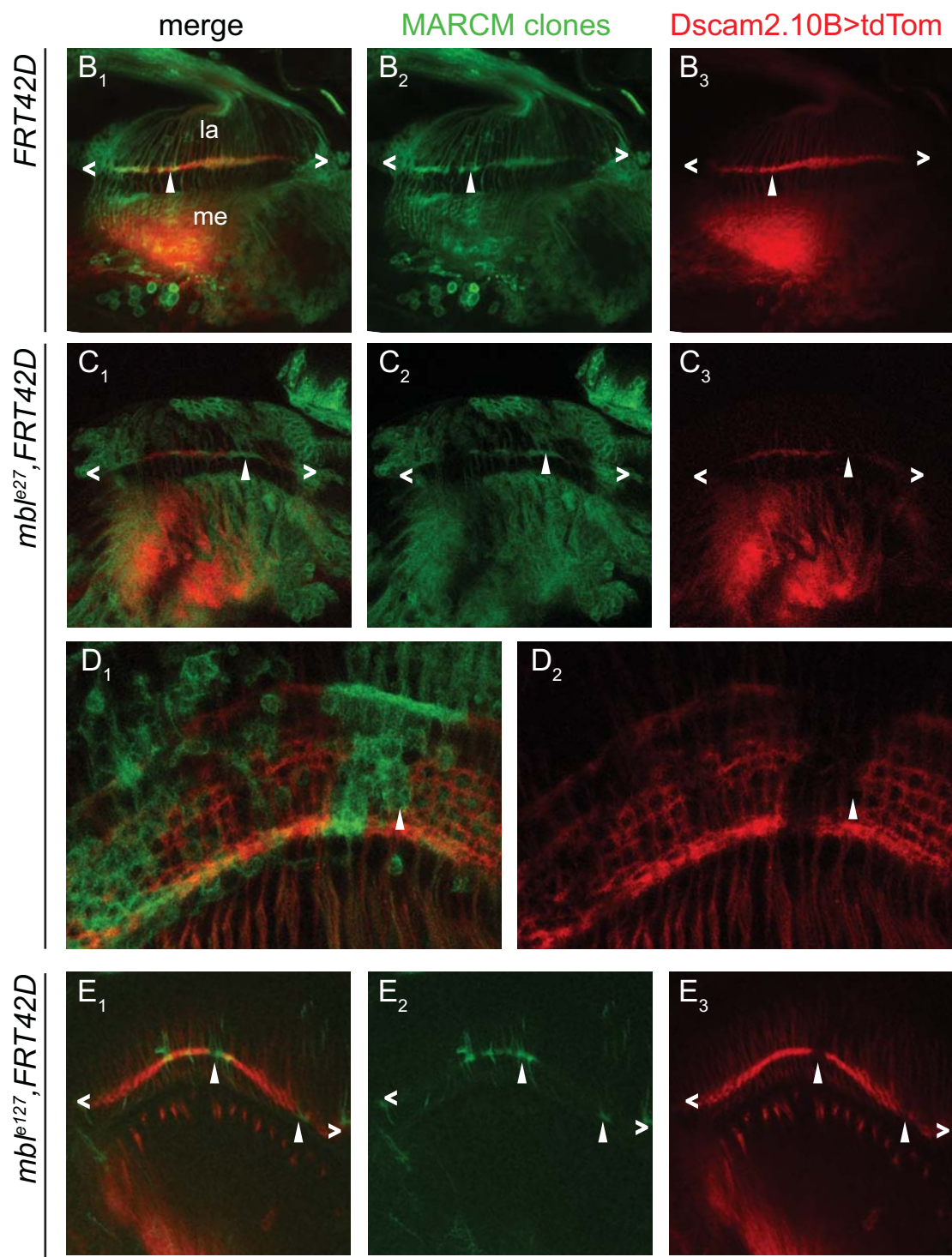
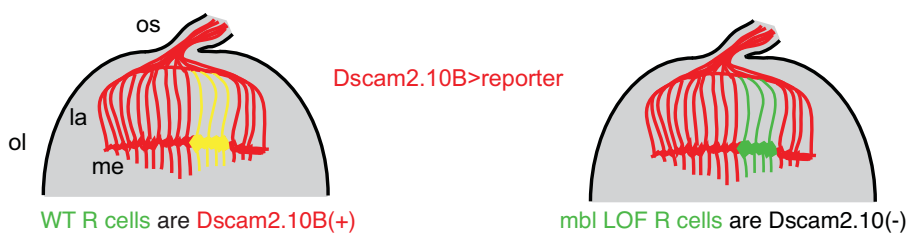
770 Wang, E.T., Sandberg, R., Luo, S., Khrebtkova, I., Zhang, L., Mayr, C., Kingsmore,  
771 S.F., Schroth, G.P., and Burge, C.B. (2008). Alternative isoform regulation in  
772 human tissue transcriptomes. *Nature* 456, 470-476.

773 Warzecha, C.C., Sato, T.K., Nabet, B., Hogenesch, J.B., and Carstens, R.P. (2009).  
774 ESRP1 and ESRP2 are epithelial cell-type-specific regulators of FGFR2 splicing.  
775 *Molecular cell* 33, 591-601.

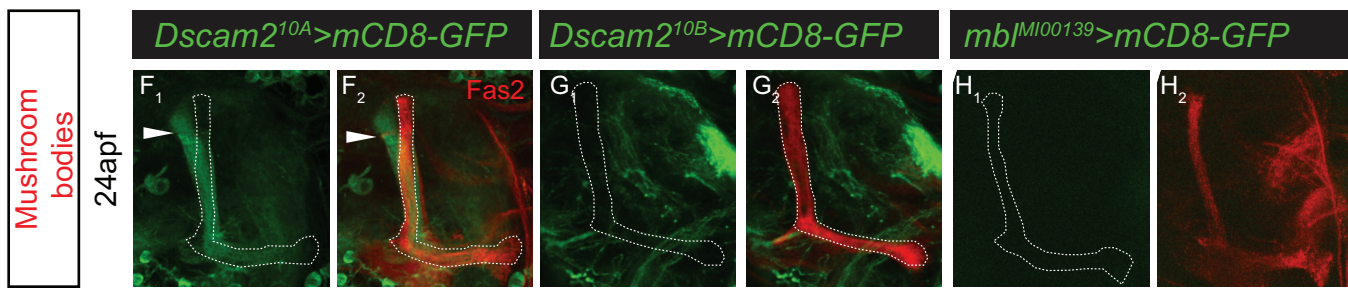
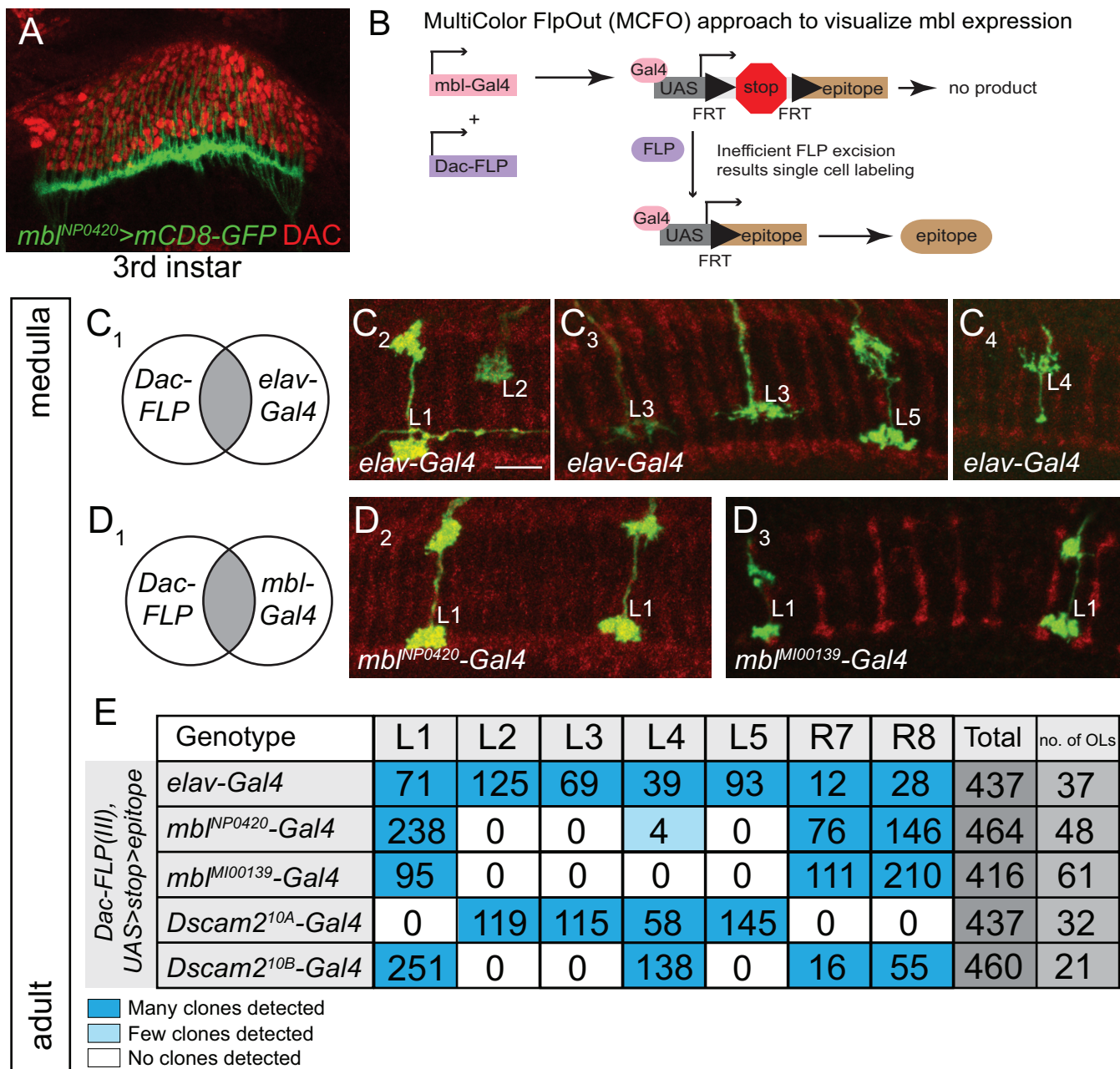
776 Xu, T., and Rubin, G.M. (1993). Analysis of genetic mosaics in developing and  
777 adult *Drosophila* tissues. *Development* 117, 1223-1237.  
778



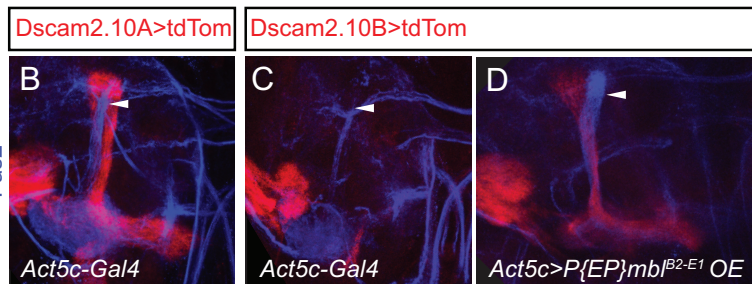
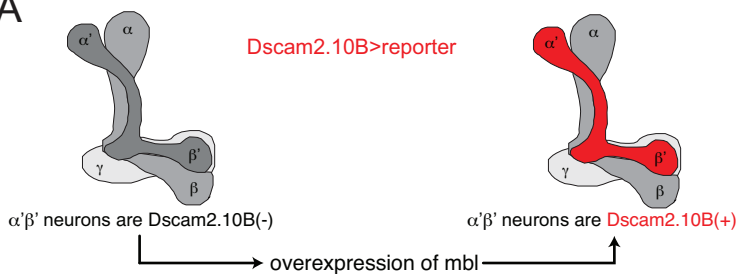
**A** ey-FLP MARCM: Mitotic recombination generates clones of *mb1* LOF R cell



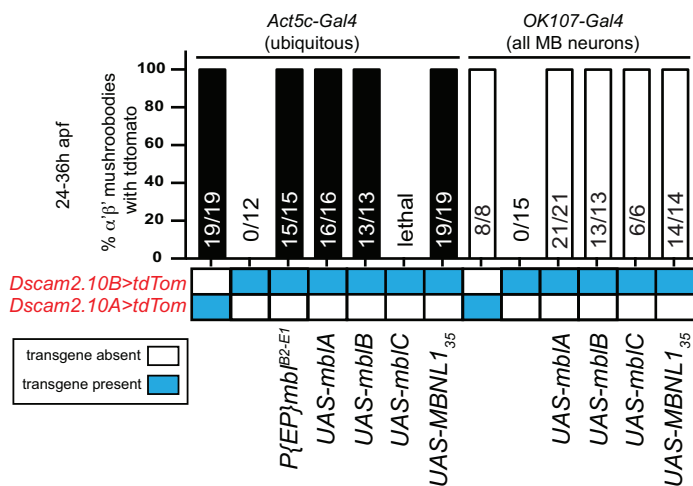




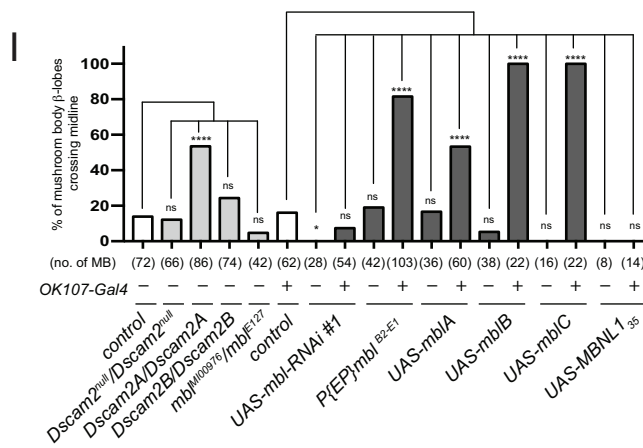
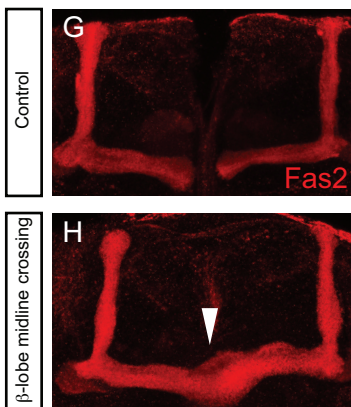
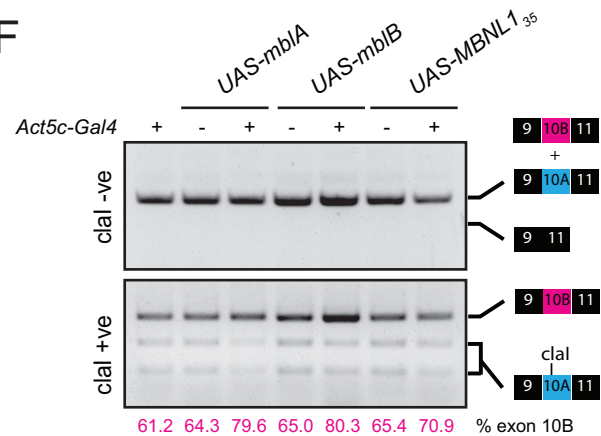
A



E



F



J

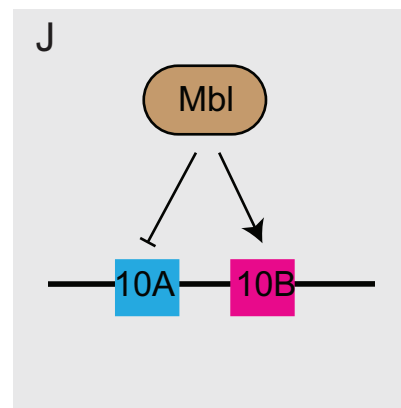


**Figure S1.** Related to Figure 1. *Mbl* LOF results in aberrant *Dscam2.10A* reporter expression in eye mosaic clones.

(A-F) Eye mosaics of *mbl* LOF alleles cause derepression of *Dscam2.10A>tdTom* in R cells. *WT* mosaic clones (GFP-negative) express *Dscam2.10B>tdTom* (A<sub>1</sub>-A<sub>4</sub>) but not *Dscam2.10A>tdTom* (B<sub>1</sub>-B<sub>4</sub>). *Mbl* mutant (GFP-negative) clones, *Df(2R)BSC154* show aberrant *Dscam2.10A* expression in R cells (C<sub>1</sub>-C<sub>4</sub>). (D) *mbl*<sup>e27</sup> eye clones exhibit derepression of *Dscam2.10A* (red). (E) Clones of a *mbl* allele that deleted only a portion of all *mbl* isoforms (*mbl*<sup>M100976</sup>) do not exhibit derepression of *Dscam2.10A*. (F) Quantification of *Dscam2.10>tdTom* expression in third instar R cells with *mbl* LOF eye mosaic clones. Y-axis represents the number of optic lobes with R cells positive for tdTom over total number of optic lobes quantified as a percentage. On the x-axis, the presence of a transgene is indicated with a blue box.

**Figure S2.** Related to Figure 1. *Mbl* LOF does not affect other *Dscam2* splicing events.

(A) *Mbl* LOF does not affect other *Dscam2* splicing events. Semiquantitative RT-PCR from different genotypes indicated. Primers amplified the variable region that includes exon 19S/19L or three alternative last exons (ALE). Percentage of 19L inclusion was calculated by dividing the 19L band by 19L+19S. Percentage of ALE 21A and ALE 21BL inclusion was calculated by dividing respectively the 21A and 21BL band by 21A+21BL+21BS (total). (B) Graphs of RT-PCR data from L. Plots show minimum (bottom line), mean (middle line) and maximum (top line) points, where individual points depict biological replicates. Dashed line represents mean of control.

**Figure S3.** Related to Figure 3. *Mbl* is expressed in R cells, neurons and glia

(A) Schematic showing the insertion locations of different *mbl* reporters. Translated regions (black) and non-translated regions (grey) are shown.

(B) *Mbl* is expressed in R cells (red) in third instar eye-discs (ed). The *mbl* splicing trap reporter (green) overlapped with a marker of R cells (24B10).

(C-G)  $mbl^{MI00139}>GFP.nls$  is expressed in neurons and muscles. (C<sub>1</sub>-C<sub>2</sub>)

Representative confocal image of a  $mbl^{MI00139}>GFP.nls$  (green) adult brain co-labelled with an ELAV antibody (red). Dashed lines demarcate GFP(+) cells. Yellow solid arrowheads show GFP(+) cells that are ELAV(-). (D) Quantification of *mbl* in third instar and adult brains where ~90-100% of GFP(+) cells are also ELAV(+) (black bars). Y-axis represents the number of GFP(+) cells positive for ELAV quantified as a percentage. (E<sub>1</sub>-E<sub>2</sub>) Representative confocal image of a  $mbl^{MI00139}>GFP.nls$  adult brain

labelled with a Repo antibody (red). Dashed lines demarcate GFP(+) cells. White solid arrowheads show GFP(+) cells that are positive for Repo. (F) Quantification of  $mbl^{MI00139}>GFP.nls$  where ~0-10% of  $mbl^{MI00139}>GFP.nls$  (+) cells are also

Repo(+). Y-axis represents the number of GFP(+) cells positive for Repo quantified as a percentage. (G<sub>1</sub>-G<sub>2</sub>)  $mbl^{MI00139}>GFP.nls$  expression is also found in third instar muscles m4-m8, m12 and m13 (Phalloidin, red).

(H<sub>1</sub>-H<sub>2</sub>) Representative confocal image of a  $mbl^{NP0420}>GFP.nls$  (green) adult brain co-labelled with an ELAV antibody (red). Dashed lines demarcate GFP(+) cells. (I)

Quantification of  $mbl^{NP0420}>GFP.nls$  in third instar and adult brains where ~80-90% of GFP(+) cells are also ELAV(+). (J-K) In third instar and adult brains,

$mbl^{NP0420}>GFP.nls$  overlaps minimally with Repo (red). (J<sub>1</sub>-J<sub>2</sub>) Representative

confocal image of a  $mbl^{NP0420}>GFP.nls$  adult brain labelled with Repo. Dashed lines demarcate GFP(+) cells. White solid arrowheads show GFP(+) cells that are positive

for Repo. (K) Quantification of  $mbl^{NP0420} > GFP.nls$  in third instar and adult brains where ~10-15% of GFP (+) cells are also Repo(+). (L<sub>1</sub>-L<sub>2</sub>)  $mbl^{NP0420} > GFP.nls$  expression is not detected in third instar muscles m4-m8, m12 and m13 (Phalloidin, red).

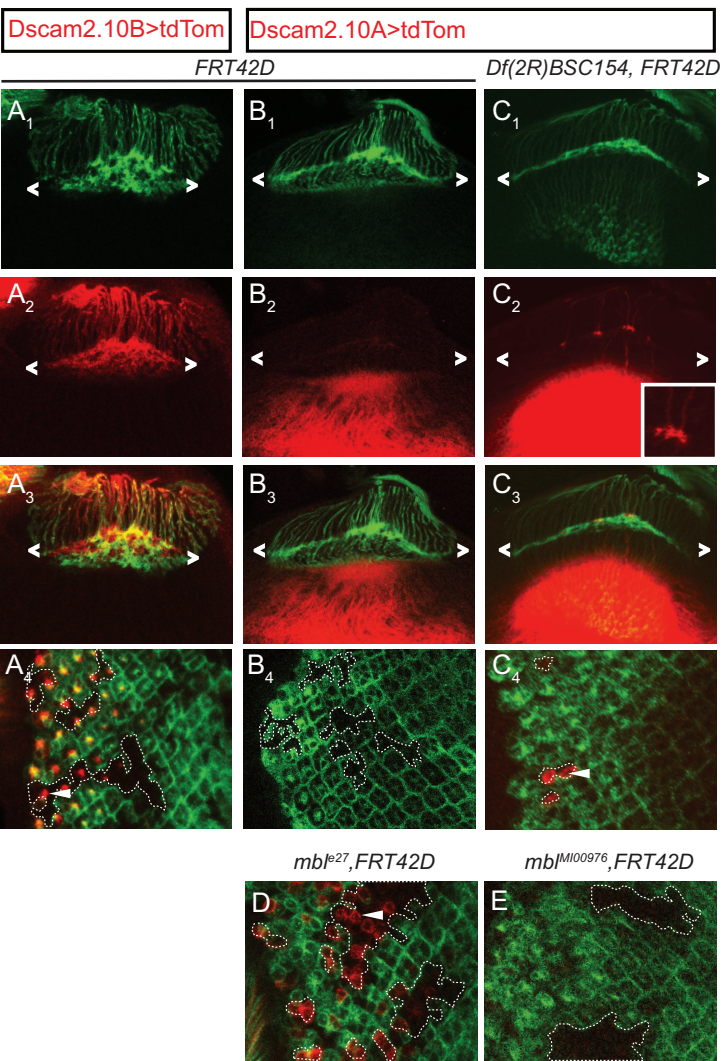
**Figure S4.** Related to Figure 3. *Mbl* expression is cell-type-specific and correlates with *Dscam2.10B*.

(A) Quantification of lamina neurons and R7-R8 neurons observed using the intersectional strategy during development. Two different *mbl* reporters were used. The transcriptional reporter labelled L4 cells early in development whereas the splicing trap reporter did not. This is most likely due to the lower efficiency of the splicing trap given that it produced 5X fewer L1 clones at 72hr compared to the transcriptional reporter. Blue boxes represent detection of reporter expression at different hours after pupal formation (apf). (B) A plot of the percentage of L4 lamina neurons over total lamina neurons during development (data from the *mbl* transcriptional reporter).

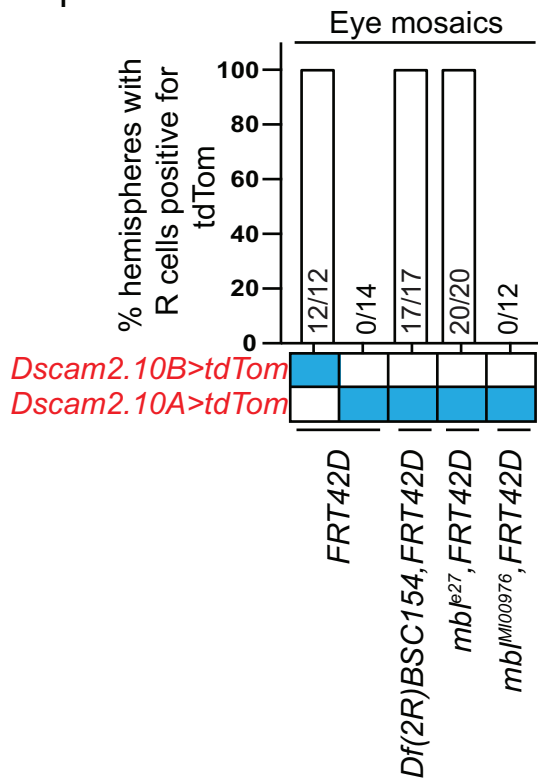
(C-E) *Mbl* is not detected in MB neurons that express *Dscam2.10A* in adults. (C<sub>1</sub>-C<sub>2</sub>) *Dscam2.10A* is expressed in  $\alpha'\beta'$  mushroom body neurons (asterisks) but not the  $\alpha\beta$  and  $\gamma$  subsets of MB neurons labelled by Fas2 (red). Neither *Dscam2.10B* (D<sub>1</sub>-D<sub>2</sub>) nor *mbl* (E<sub>1</sub>-E<sub>2</sub>) are expressed in MB neurons. Neurons in the midline express both *Dscam2.10B* and *mbl* (white arrowhead).



3rd instar  
Eye mosaics (ey-FLP)

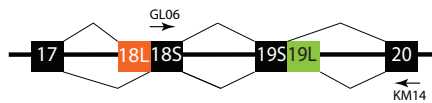


F

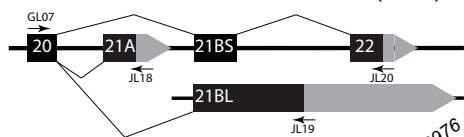


A

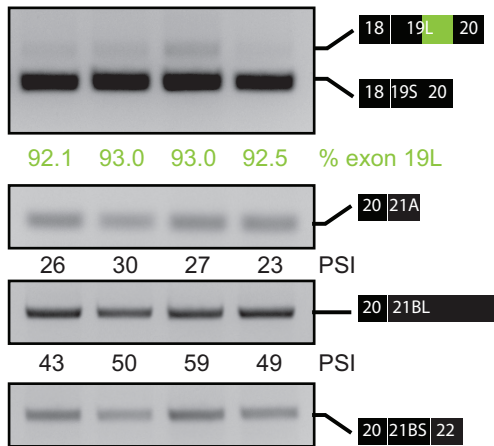
Dscam2 exon 19S/19L



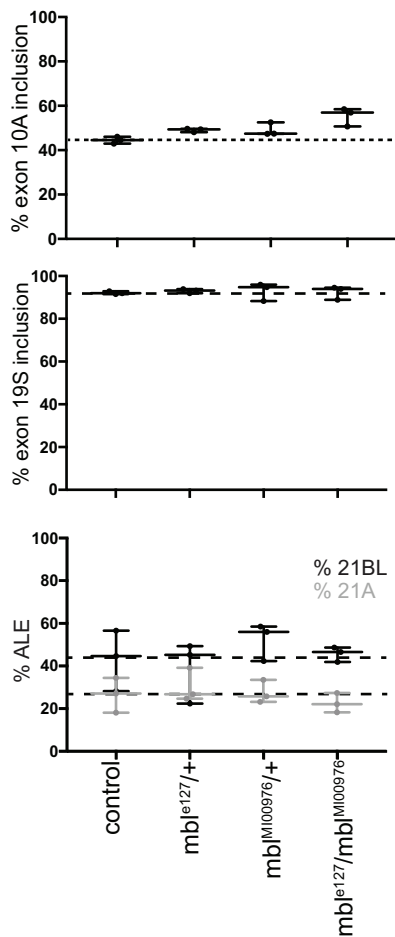
Dscam2 alternative last exons (ALE)

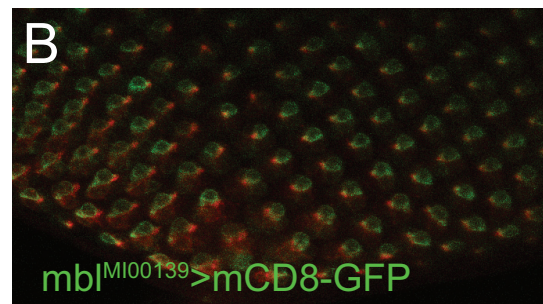
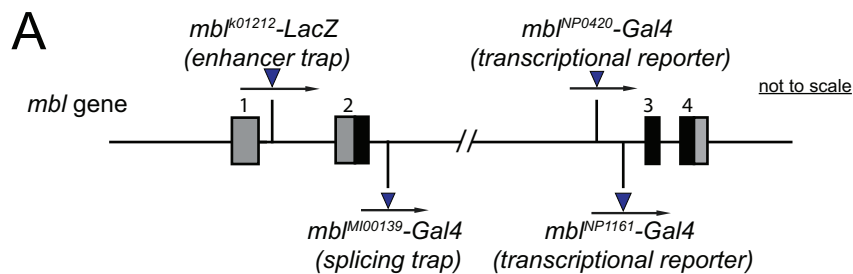


control

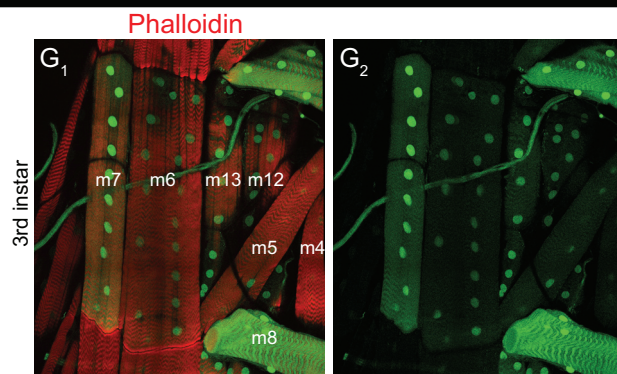
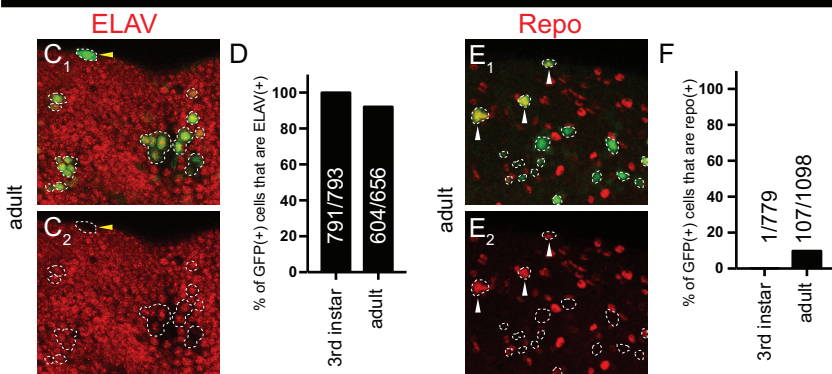
 $mbj^{e127/+}$  $mbj^{M100976/+}$  $mbj^{e127}/mbj^{M100976}$ 

B

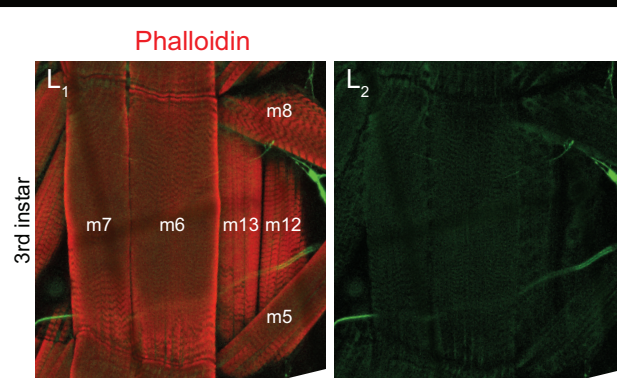
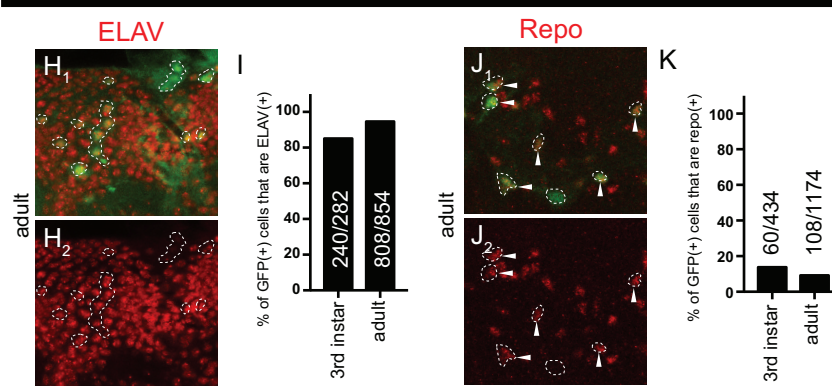




*mbI*<sup>MI00139</sup>>GFP.nls




*mbI*<sup>NP0420</sup>>GFP.nls



A

Genotype		L1	L2	L3	L4	L5	R7	R8	Total	no. of OLS
<i>Dac-FLP(III), UAS&gt;stop&gt;epitope</i>	<i>mbI<sup>NP0420</sup>-Gal4</i> 72 apf	75	0	0	10	0	10	38	133	8
	<i>mbI<sup>NP0420</sup>-Gal4</i> 60 apf	22	0	0	8	0	15	29	74	8
	<i>mbI<sup>NP0420</sup>-Gal4</i> 48 apf	7	0	0	3	0	1	9	20	2
<i>mbI<sup>MI00139</sup>-Gal4</i>	72 apf	15	0	0	0	0	6	15	36	8
	48 apf	12	0	0	0	0	4	24	40	8

 Clones detected

 No clones detected

B

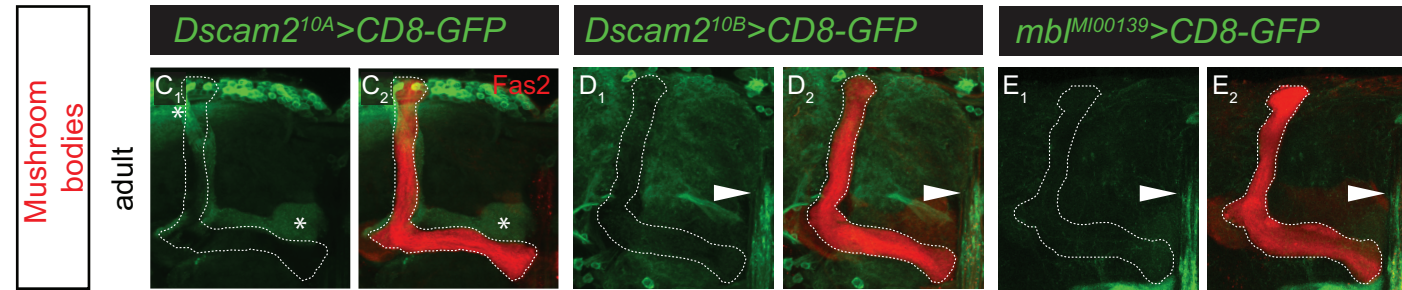
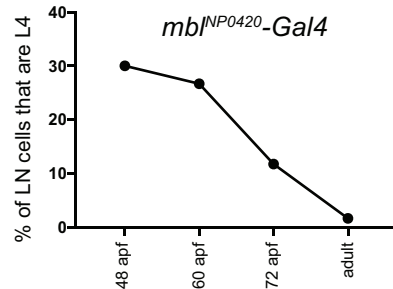


Table S1. List of tested RNAi that did not de-repress Decam2 exon 10A in R cells

Flybase Number	CG Number	Gene Name	RNAi ID	no. of oilied	no. of animals	Flybase Number	CG Number	Gene Name	RNAi ID	no. of oilied	no. of animals	Flybase Number	CG Number	Gene Name	RNAi ID	no. of oilied	no. of animals
FBgn0052062	CG32062	A2bp1	Z7286	12	6	FBgn0024698	CG10110	Cpsf160	v18009	11	6	FBgn0260944	CG17136	Rbp1	v110008	11	6
FBgn026239	CG6671	AGO1	33727	3	2	FBgn0024698	CG10110	Cpsf160	v110571	9	6	FBgn0030479	CG1987	Rbp1-like	v105883	10	6
FBgn0000114	CG31762	aret	44483	18	9	FBgn0261065	CG7698	Cpsf73	v39558	9	5	FBgn0030479	CG1987	Rbp1-like	44100	4	2
FBgn0004587	CG10851	B52	v38862	16	8	FBgn0000377	CG3193	crm	v25919	lethal		FBgn0260943	CG32169	rbp6	61324/CyOtb	8	4
FBgn0004587	CG10851	B52	v38860	4	2	FBgn0039867	CG2261	Caif-50	v43716	10	5	FBgn0015778	CG9412	rin	v3392/TM6B	12	7
FBgn0037660	CG18005	beag	v103832	8	4	FBgn0039867	CG2261	Caif-60	v109583	8	4	FBgn0003261	CG10279	Rm62	v46908/TM6B	12	6
FBgn0015907	CG13425	bl	v2912	10	6	FBgn0027841	CG7697	Caif-64	v210451/CyOtb	10	6	FBgn0037707	CG16788	RnpS1	56910	10	5
FBgn0015907	CG13425	bl	v105271	9	5	FBgn0010220	CG12759	Dbp45A	v17306	6	3	FBgn0037707	CG16788	RnpS1	36580	6	3
FBgn0262475	CG6319	bru-2	50631	13	7	FBgn0010220	CG12760	Dbp45A	v104183	13	7	FBgn0005649	CG5422	Rox8	v100563	10	5
FBgn0264001	CG43744	Bru-3	50734	8	4	FBgn0033160	CG11107	Dhx15	v441191/CyOtb	10	6	FBgn0005649	CG5422	Rox8	v41439	12	6
FBgn0031883	CG11266	Caper	55742	10	6	FBgn0031601	CG3058	Dim1	v21258	10	5	FBgn0011305	CG5655	Rsf1	v22186/TM3	15	10
FBgn0031883	CG11266	Caper	55742	8	4	FBgn0259220	CG42320	Doa	v19066	9	5	FBgn0267790	CG9373	rump	42665/CyOtb	6	3
FBgn0022942	CG7035	Cbp80	v22331	12	8	FBgn0020306	CG9696	dom	v7787	2	1	FBgn0039229	CG6995	Saf-8	51759	5	5
FBgn0035136	CG6905	Cdc5	v13492	2	1	FBgn0000562	CG4051	egl	28969	8	4	FBgn0265298	CG5442	SC35	v40590	5	3
FBgn0035136	CG6905	Cdc5	v109369	10	5	FBgn0001942	CG9075	elf-4A	v42202	lethal		FBgn0265298	CG5442	SC35	v104928	6	3
FBgn00032690	CG10333	CG10333	v18132	12	8	FBgn0034237	CG4878	elf3-59	32880	lethal		FBgn0025571	CG5836	SF1	v13426	3	2
FBgn00032690	CG10333	CG10333	v18133	4	2	FBgn0260400	CG4262	elav	28371	2	1	FBgn0040284	CG6987	SF2	v27775/TM3	13	7
FBgn0036277	CG10418	CG10418	v105940	11	6	FBgn0033859	CG6197	fand	v104186	10	5	FBgn0040284	CG6987	SF2	v27776/TM6B	6	4
FBgn0037531	CG10445	CG10445	v104753	14	7	FBgn0036850	CG10419	Gem2	v47372	13	8	FBgn0052423	CG32423	shep	43545	4	3
FBgn0036314	CG10754	CG10754	v31346	11	8	FBgn0036850	CG10419	Gem2	v47374	10	7	FBgn0002354	CG1420	Su7	v103587	5	3
FBgn0039920	CG11360	CG11360	v38491	15	8	FBgn0259139	CG6946	glo	33668	9	6	FBgn0262601	CG5352	SmB	v40587	3	2
FBgn0039920	CG11360	CG11360	v38492	11	6	FBgn0259139	CG6946	glo	v27752	12	6	FBgn0262601	CG5352	SmB	v110713	12	6
FBgn0035692	CG13298	CG13298	55257	8	4	FBgn0001179	CG8019	hay	v41023	12	8	FBgn0261933	CG10753	SmD1	v31343/TM6B	8	4
FBgn0035162	CG13900	CG13900	v18955	9	6	FBgn0014189	CG7269	Hel25E	v22557	9	5	FBgn0261933	CG10753	SmD1	v31342	7	4
FBgn0035163	CG13900	CG13900	v108248	16	8	FBgn0011224	CG31000	heph	v37375	10	6	FBgn0261789	CG1249	SmD2	v31947	4	2
FBgn0037220	CG14641	CG14641	v110507/CyOtb	11	6	FBgn0011224	CG31000	heph	v110749	18	10	FBgn0261789	CG1249	SmD2	v31946	8	4
FBgn0038464	CG16941	CG16941	v20338	1	1	FBgn0264491	CG10293	how	v13756	13	7	FBgn0261789	CG1249	SmD2	v100690	4	2
FBgn0033089	CG17266	CG17266	v25243	10	5	FBgn0264491	CG10293	how	v100775	10	5	FBgn0023167	CG8427	SmD3	v35933	8	5
FBgn0033089	CG17266	CG17266	v25244	2	1	FBgn0004838	CG10377	Hrb27c_Hrp48	v16040	12	7	FBgn0261790	CG18591	SmE	v23569	4	2
FBgn0029751	CG17764	CG17764	v20541	12	7	FBgn0004838	CG10377	Hrb27c_Hrp48	31685	6	3	FBgn0261790	CG18591	SmE	v23570/TM6B	10	5
FBgn0029751	CG17764	CG17764	v101894	10	5	FBgn0004838	CG10377	Hrb27c_Hrp48	33716	8	4	FBgn000426	CG16792	SmF	v107644/CyOtb	lethal	
FBgn0035271	CG2021	CG2021	28579	8	5	FBgn0004237	CG12749	Hrb87F_hrp36	v51759	9	6	FBgn000426	CG16792	SmF	26734	12	6
FBgn0031266	CG2807	CG2807	v25162	8	5	FBgn0004237	CG12749	Hrb87F_hrp36	52937	11	6	FBgn0036641	CG16725	Smm	v100392	7	4
FBgn0037344	CG2926	CG2926	v33589	11	5	FBgn0004237	CG12749	Hrb87F_hrp36	31244	14	8	FBgn0003449	CG4528	snf	51549	16	8
FBgn050122	CG30122	CG30122	55209	6	3	FBgn0001215	CG9983	Hrb98DE_hrp38	31303	10	7	FBgn0003449	CG4528	snf	55914	9	5
FBgn0031631	CG3225	CG3225	v24725	9	5	FBgn0001215	CG9983	Hrb98DE_hrp38	32351	13	8	FBgn0016978	CG8749	snRNP-U1-70K	v23150	11	8
FBgn0052533	CG32533	CG32533	v38634	1	1	FBgn0015949	CG9854	hrg	v42283	12	6	FBgn0016978	CG8749	snRNP-U1-70K	v23151	10	6
FBgn0052533	CG32533	CG32533	v51785	11	6	FBgn0002431	CG9844	hyd	v44675	12	6	FBgn0261792	CG5654	snRNP-U1-C	v22132	11	6
FBgn0031628	CG3294	CG3294	v26111/TM6B	12	6	FBgn0039691	CG1972	IntS11	v33450	7	5	FBgn0261792	CG5654	snRNP-U1-C	v22133	10	5
FBgn0031628	CG3294	CG3294	v26111/TM6B	11	6	FBgn0039691	CG1972	IntS11	v109408	8	5	FBgn0261791	CG9742	SNRPG	v39256	10	5
FBgn0053108	CG33108	CG33108	v24996	9	5	FBgn0036570	CG5222	IntS9	v110367	10	5	FBgn0015818	CG3780	Spx	v40471	9	5
FBgn0031229	CG3436	CG3436	55207/CyOtb	4	2	FBgn0026713	CG32604	(1)YG007	v31909	15	8	FBgn0015818	CG3780	Spx	v40472	9	5
FBgn0031492	CG3542	CG3542	v26227	10	5	FBgn0026714	CG32605	(1)YG008	v31909	4	2	FBgn0263396	CG16901	squ_hrp40	v32395	12	6
FBgn0031492	CG3542	CG3542	v26229	4	2	FBgn0086444	CG10689	(2)37Cb	v31324	9	6	FBgn0263396	CG16901	squ_hrp40	31302	20	10
FBgn0031493	CG3605	CG3605	v26250	12	7	FBgn0263599	CG5931	(3)J72Ab	v43962	5	3	FBgn0036340	CG11274	Srm160	v6439	9	5
FBgn0031493	CG3605	CG3605	v26252	8	5	FBgn0263600	CG5932	(3)J72Ab	v110666	6	3	FBgn0036340	CG11274	Srm160	v100715	8	4
FBgn0035987	CG3689	CG3689	v45278	8	5	FBgn0035838	CG7942	ldtr	v110582	8	5	FBgn0015298	CG4457	Srp19	51600	lethal	
FBgn0028474	CG4119	CG4119	v28305	9	5	FBgn0035838	CG7942	ldtr	55661	8	6	FBgn0024285	CG4602	Srp54	v51088	8	6
FBgn0028474	CG4119	CG4119	v106696/CyOtb	10	6	FBgn0034834	CG3162	LS2	v21379	11	7	FBgn0024285	CG4602	Srp54	55254	9	5
FBgn0034598	CG4266	CG4266	v26472	14	7	FBgn0034834	CG3162	LS2	v21380	14	7	FBgn0026370	CG8174	SRPK	v103416	9	6
FBgn0034598	CG4266	CG4266	v26475	4	2	FBgn0261067	CG4279	Lsm11	v28793	11	6	FBgn0025702	CG11489	srpk79D	v47544	8	5
FBgn0031287	CG4291	CG4291	v21819/TM6B	11	6	FBgn0261067	CG4279	Lsm11	v50653	10	5	FBgn0025702	CG11489	srpk79D	v45455	10	5
FBgn0030516	CG4612	CG4612	v52497	9	5	FBgn0033450	CG12924	Lsm11	v108336	12	6	FBgn0003520	CG5753	stau	31247	9	5
FBgn0030566	CG4849	CG4849	v21962	9	5	FBgn0051184	CG31184	Lsm3	v56892	4	2	FBgn0003559	CG17170	su(f)	610125	6	3
FBgn0032194	CG4901	CG4901	v34904	11	6	FBgn0261068	CG13277	Lsm7	v23862	10	6	FBgn0003638	CG3019	su(wa)	v25597	12	9
FBgn0038344	CG5205	CG5205	v107282	9	5	FBgn0011666	CG5099	msi	55152	10	5	FBgn0003638	CG3019	su(wa)	v104716	10	5
FBgn0039182	CG5728	CG5728	v24697	14	7	FBgn0262737	CG7437	mub	v28024	16	9	FBgn0264270	CG43770	Sxl	v34393	10	5
FBgn0038927	CG6015	CG6015	34565	lethal		FBgn0014366	CG2925	noi	v20943	9	5	FBgn0037371	CG2097	Syp	v33470	9	5
FBgn0030631	CG6227	CG6227	v40351	11	8	FBgn0015520	CG10328	non-A1	v101567	7	4	FBgn0038826	CG17838	symp	56972	10	5
FBgn0030632	CG6227	CG6227	v40352	12	6	FBgn0015520	CG10328	non-A1	52934	3	2	FBgn0038826	CG17838	symp	v33012	15	9
FBgn0004903	CG6354	CG6354	31333	12	9	FBgn0261619	CG5119	pAbp	v22007	9	5	FBgn0025790	CG10327	TBPH	v38377	7	4
FBgn0004903	CG6354	CG6354	55662	8	4	FBgn0005648	CG2163	Pabp2	v106466	10	5	FBgn0025790	CG10327	TBPH	v38379	10	5
FBgn0035675	CG6610	CG6610	v106830	10	6	FBgn0086895	CG8241	pea	v47782	9	5	FBgn0003741	CG16724	tra	v2560	12	6
FBgn0035675	CG6610	CG6610	31870	10	6	FBgn0027784	CG6011	Prp18	v13760	10	7	FBgn0003742	CG10128	tra2	v8888	9	5
FBgn0038828	CG6841	CG6841	v34253/CyOtb	10	5	FBgn0027784	CG6011	Prp18	v100287	2	1	FBgn0039117	CG10210	tsst	v38562	8	4
FBgn0030085	CG6999	CG6999	v110143	11	7	FBgn0261119	CG5519	Prp19	v108575	11	6	FBgn0039117	CG10210	tsst	v108216	12	6
FBgn0030085	CG6999	CG6999	55157	12	6	FBgn0261119	CG5519	Prp19	v41438	3	2	FBgn0033378	CG8781	tsu	55367	11	6
FBgn0035872	CG7185	CG7185	v107147	5	3	FBgn0036915	CG7757	Prp3	v25548	9	6	FBgn0033378	CG8781	tsu	28955	9	5
FBgn0035872	CG7185	CG7185	34804	14	7	FBgn0036487	CG6876	Prp3	v35131	3	2	FBgn0033210	CG1406	U2A	v17358/TM6B	9	5
FBgn0036734	CG7564	CG7564	v100562	10	5	FBgn0036487	CG6876	Prp3	v103721	12	7	FBgn0033210	CG1406	U2A	v109815		